FEMS Microbiology Ecology, 97, 2021, fiab033

doi: 10.1093/femsec/fiab033
Advance Access Publication Date: 20 February 2021
Research Article

RESEARCH ARTICLE

Crop type exerts greater influence upon rhizosphere phosphohydrolase gene abundance and phylogenetic diversity than phosphorus fertilization

Andrew L. Neal[1,†], Timothy McLaren[2], Mariana Lourenço Campolino[3,4], David Hughes[5], Antônio Marcos Coelho[4], Ubiraci Gomes de Paula Lana[4], Eliane Aparecida Gomes[4] and Sylvia Morais de Sousa[3,4,*,‡]

[1]Department of Sustainable Agricultural Sciences, Rothamsted Research, North Wyke, Devon EX20 2SB, UK, [2]Department of Environmental Systems Science, Swiss Federal Institute of Technology (ETH) Zürich, Eschikon 33, 8315 Lindau, Switzerland, [3]Universidade Federal de São João del-Rei, Bioengineering, R. Padre João Pimentel, 80 - Dom Bosco, São João del-Rei, Minas Gerais, 36301-158, Brazil, [4]Empresa Brasileira de Pesquisa Agropecuária, Embrapa Milho e Sorgo, Rod MG 424 Km 65, Sete Lagoas, Minas Gerais, 35701-970, Brazil and [5]Department of Computational and Analytical Sciences, Rothamsted Research, Harpenden, Hertfordshire AL5 2JQ, UK

*Corresponding author: Empresa Brasileira de Pesquisa Agropecuária, Embrapa Milho e Sorgo, Rod MG 424 Km 65, Sete Lagoas, Minas Gerais, 35701-970, Brazil. Tel: +55-31-3024-1904; E-mail: sylvia.sousa@embrapa.br

One sentence summary: Rhizospheres of maize and sorghum harbor different assemblages of phosphohydrolase gene ecotypes.

Editor: Carolina Leoni

†Andrew L. Neal, http://orcid.org/0000-0003-4225-1396
‡Sylvia Morais de Sousa, http://orcid.org/0000-0002-8030-1385

ABSTRACT

Rock phosphate is an alternative form of phosphorus (P) fertilizer; however, there is no information regarding the influence of P fertilizer sources in Brazilian Cerrado soils upon microbial genes coding for phosphohydrolase enzymes in crop rhizospheres. Here, we analyze a field experiment comparing maize and sorghum grown under different P fertilization (rock phosphate and triple superphosphate) upon crop performance, phosphatase activity and rhizosphere microbiomes at three levels of diversity: small subunit rRNA marker genes of bacteria, archaea and fungi; a suite of alkaline and acid phosphatase and phytase genes; and ecotypes of individual genes. We found no significant difference in crop performance between the fertilizer sources, but the accumulation of fertilizer P into pools of organic soil P differed. Phosphatase activity was the only biological parameter influenced by P fertilization. Differences in rhizosphere microbiomes were observed at all levels of biodiversity due to crop type, but not fertilization. Inspection of phosphohydrolase gene ecotypes responsible for differences between the crops suggests a role for lateral genetic transfer in establishing ecotype distributions. Moreover, they were not reflected in microbial community composition, suggesting that they confer competitive advantage to individual cells rather than species in the sorghum rhizosphere.

Received: 23 April 2020; **Accepted:** 18 February 2021

Keywords: phosphatase; phytase; Cerrado; metagenomics; microbiome; maize; sorghum

INTRODUCTION

Due to areas sown and annual production volume, cereals play an important role in human nutrition, as food and animal feed, and in the world's agricultural economy. Maize, wheat and rice are the most widely produced grains, but crops such as sorghum are especially important in Africa (FAO 2019). The world's current population of around 7 billion is estimated to exceed 9 billion by 2050. Challenges to feed an ever-growing human population—within the context of global climate change—increase the need for adoption of sustainable and environmentally sound agricultural practices (Ngumbi and Kloepper 2016; Naumann *et al.* 2018; FAO 2019).

Factors that constrain soil fertility and thus, sustainable agriculture, in the tropics are typically low-nutrient capital, water stress, erosion, high phosphorus (P) sorption and high acidity allied to aluminum toxicity (Camenzind *et al.* 2018; Garland *et al.* 2018). Soluble P fertilizers applied to soil are often rapidly complexed via adsorption to iron and aluminum oxides, particularly in clayey tropical soils typical of Cerrado and other Savannah areas worldwide. Such complexation reduces the bioavailability of the added P to plants (Novais and Smyth 1999). P can also be complexed to or within organic compounds that may represent as much as 80% of the total P in no-till soils (Marschner, Solaiman and Rengel 2006). As a result of these processes, organic P pools and decomposition of soil organic matter are critical for sustainable plant productivity in highly weathered tropical soils. The origin, distribution and abundance of genes coding for various families of enzymes associated with the hydrolysis of organic P pools (several families of alkaline and acid phosphatases and phytases) in soils are not particularly well understood, neither is the effect of fertility management upon gene dynamics (George *et al.* 2018).

Chemical fertilizers, such as manufactured water-soluble phosphate, traditionally play a significant role in maintaining pools of bioavailable P in managed agricultural soils. Rising demand for food in developing countries is in turn exerting increased pressure on agricultural land for higher yields and thus increased demand for phosphate fertilizers, leading to an increase in global fertilizer price inflation. Resource-poor farmers are faced with poor-yielding soils that defy costly attempts to improve their nutrient status by fertilization. This places individual, community and national food security at risk. In addition, intensive use of agricultural inputs can cause environmental impacts, such as pollution, soil degradation, micronutrient deficiency, eutrophication of water sources, toxicity to different beneficial organisms and reduction of microbiota biodiversity (Sharma and Singhvi 2017).

In response to these issues, much research has been directed to understanding the role of rock phosphate (RockP) fertilizers in agroecosystems, as it has a relatively low cost and is environmentally less damaging than soluble P (Chien *et al.* 2011). Despite its lower reactivity compared with soluble fertilizers, the P bioavailability of RockP can increase over years of cultivation, due to physicochemical processes and the activity of soil microbiota (Silva *et al.* 2017). Phosphate solubilizing and mineralizing microorganisms have a high potential to be used in the management of P-deficient soils, since they can liberate adsorbed P as a bi-product of organic acid production, and chelate Al and Fe, reducing the precipitation of phosphate minerals (Vega 2007). Many tropical soils naturally support high microbiological activity and biodiversity—much of it is underexplored. This diversity could be exploited to counter the challenges associated with food production in highly weathered tropical soils (Cardoso and Kuyper 2006).

Plant roots exude organic compounds, including sugars, organic acids, nucleosides, mucilage and amino acids. The resulting concentration gradients can attract microorganisms from the bulk soil to the rhizosphere and to the endosphere (Edwards *et al.* 2015) as well as support higher growth. Plant species exert a strong influence upon rhizosphere microbiomes, but other factors such as soil properties, fertilizers, plant developmental stages, nutritional status of the host plant and other environmental factors can have confounding effects on rhizosphere microbial communities (Mota *et al.* 2008; Li *et al.* 2014; Bakker *et al.* 2015). Previous work on Brazilian Oxisol Cerrado soils demonstrated that a significant fraction of bacterial and fungal diversity is attributed to the plant host genotype, but in general, the soil P status was the major driver of microbiome structure followed by plant compartment (rhizosphere versus rhizoplane associated) (Gomes *et al.* 2018). This work tested the hypothesis that because of their different reactivities and resulting availability of orthophosphate, fertilization with highly reactive triple superphosphate (TSP) would result in lower abundances of microbial phosphatase and phytase genes in crop rhizospheres compared with less reactive rock phosphate. To test this hypothesis, we investigated the (i) P chemistry in soils of a tropical P fertilizer field trial comparing different sources of P fertilization; (ii) phosphatase activity under different crop and fertilizer regimes and (iii) the biodiversity of microbial phosphohydrolase genes involved in organic P cycling.

MATERIALS AND METHODS

Site description and soil preparation

The fertilization regimes were established in 2017 in a soil fallowed since 2007 at Embrapa Milho e Sorgo Experimental Station in Sete Lagoas, Minas Gerais, Brazil (19°28′S, 44°15′W at an altitude of 732 m above sea level). The soil is classified as a Distroferric Red Latosol (Latossolo Vermelho Distroférrico) with a clayey texture (Oxisol), under Savannah vegetation (Santos *et al.* 2013) and a pH (H_2O) of 5.9 in the surface layer (0–20 cm). The experiment was under no-till soil management with irrigation when necessary of two continuous crops: sorghum [*Sorghum bicolor* (L.) Moench] and maize (*Zea mays* L.). The field experiment consisted of three fertilizer treatments: (i) plots without addition of fertilizer P (P0, unfertilized soil treatment); (ii) plots receiving rock phosphate (RockP) (18% total P_2O_5 and 4% soluble in a 2% citric acid solution) at a rate of 100 kg of P_2O_5 ha^{-1} and (iii) plots receiving triple superphosphate (TSP) (45% total P_2O_5) at a rate of 100 kg of P_2O_5 ha^{-1} $year^{-1}$. Soil was sampled in the second season of the experiment (2018/2019), after fertilized plots had received ~44 kg-P ha^{-1} yr^{-1} or a cumulative 88 kg-P ha^{-1}. Prior to establishment of the experiment, the field was fallowed under a natural *Brachiaria* pasture between 2007 and 2017. Crops were fertilized at sowing with 40 kg-N ha^{-1} and 60 kg-K_2O ha^{-1} and then again as a side dress 30–35 days after planting with 120 kg-N ha^{-1} and 60 kg-K_2O ha^{-1}. Micronutrients were not applied because soil analyses indicated that they were at sufficient levels.

The experimental design was a randomized complete block with three replications. For soil samples, the cropped areas of maize or sorghum were each divided in 10 blocks measuring 20 m wide × 18 m long. Soil samples were obtained in August 2017: five subsamples were collected to a depth of 20 cm for each block to form a composite sample. Measured soil parameters, according to Embrapa (1997), were: potential acidity (H+Al) = 7.36; calcium (Ca) = 3.03 mg dm^{-3}; magnesium (Mg) = 0.47 mg dm^{-3}; cation exchange capacity = 10.99 $cmol_c$ dm^{-3}; Mehlich-1 extractable P = 5.16 mg dm^{-3}; potassium (K) = 53.8 mg dm^{-3}; base saturation = 33.4% and organic matter (OM) = 36.9 g kg^{-1}. During flowering in 2018/2019, rhizosphere soil was collected from the fine roots of four plants of each crop from each of triplicate treatment plots. After removing weakly adhered soil by manual brushing, 10 g of rhizosphere soil was weighed and frozen in liquid nitrogen. Additional soil from the surface (0–20 cm) was sampled, dried and sieved prior to chemical analyses. At cropping, maize cobs and sorghum panicles from the inner crop lines were harvested and threshed by subplot. The resulting grain mass was weighed and corrected for 130 g kg^{-1} grain moisture to estimate the total grain yield in Mg ha^{-1}.

Soil organic phosphorus

Soil organic P was estimated using the method of Cade-Menun and Preston (1996). A total of 2 g of soil was extracted with 40 mL of 0.25 M NaOH + 0.05 M Na_2-EDTA solution using a horizontal shaker at 160 rpm for 16 h. The extracts were then centrifuged at 5000 rpm for 20 min, and the supernatant passed through a Whatman no. 42 filter paper (Sigma-Aldrich, Saint Louis, MO, USA). A 20 mL aliquot of the filtrate was frozen at −80°C, lyophilized and weighed (Doolette, Smernik and Dougherty 2010). This resulted in a mass of lyophilized material ranging from 560 to 574 mg per tube across all samples.

Solution phosphorus-31 nuclear magnetic resonance (NMR) spectroscopy

Preparation of lyophilized material for solution ^{31}P NMR analysis has been described by Reusser *et al.* (2020). Solution ^{31}P NMR spectroscopy was carried out on one replicate of each treatment using a Bruker Avance III HD 500 MHz NMR spectrometer equipped with a 5 mm liquid-state Prodigy CryoProbe (Bruker Corporation, Billerica, MA, USA) at the NMR facility of the Laboratory of Inorganic Chemistry (Hönggerberg, ETH Zürich). Solution ^{31}P NMR spectra were acquired at a ^{31}P frequency of 202.5 MHz and gated broadband proton decoupling with 90° pulses of 12 μs duration. Spectral resolution was <0.1 Hz following sample shimming across all samples. Two NMR analyses were carried out on all soil samples. The first was an inversion recovery experiment (Vold *et al.* 1968) to obtain the spin-lattice relaxation (T_1) times of the ^{31}P NMR signal. The longest T_1 time for each soil sample was multiplied 5-fold and used as the recycle delay of the subsequent ^{31}P (1D) NMR analysis. Spin-lattice relaxation times were the longest for orthophosphate across all soil samples, which ranged from 17 to 29 s. The average number of scans across all soil samples was 3754.

Spectral quantification and identification of peaks

All NMR spectra were initially processed with TopSpin® software (Bruker Corporation, Billerica, MA, USA), which involved spectral phasing and baseline correction. Furthermore, the net peak areas (integrals) of all ^{31}P NMR signals were obtained. This generally occurred in the phosphonate region (δ 22.02 to 21.98 ppm, 19.81 to 19.76 ppm, 17.02 to 16.31 ppm and 14.32 to 14.25 ppm), the combined orthophosphate and phosphomonoester regions (δ 6.10 to 2.62 ppm), the phosphodiester region (δ 0.98 to 0.94 and −0.73 to −1.43 ppm) and the polyphosphate region (δ −4.85 to −4.94 ppm). The integral of the NMR signal between δ 17.02 and 16.31 ppm was that of the added MDP (δ 16.67 ppm), including its two ^{13}C satellite peaks (δ 16.96 ppm and 16.37 ppm). Due to overlapping peaks in the combined orthophosphate and phosphomonoester region, spectral deconvolution and peak fitting was used to partition the NMR signal, following procedures described by Reusser *et al.* (2020). This involved fitting the region with between 23 and 50 sharp signals and one broad signal across all samples. Inositol phosphates were identified by spiking and comparison of spectra to previously spiked soil extracts using purchased reference materials and compounds from original collections of Dr Dennis Cosgrove and Dr Max Tate. The assignment of the broad signal was based on spiking experiments (Reusser *et al.* 2020), transverse relaxation (T_2) experiments (McLaren, Verel and Frossard 2019) and its isolation in large molecular weight material (McLaren *et al.* 2015).

Quantitative solution ^{31}P NMR spectra were obtained based on recycle delays allowing for complete relaxation of ^{31}P nuclei between pulses, and the addition of a known quantity of P as MDP that has a chemical shift separate to that of all other NMR signals in these soil samples. The net peak area of MDP is directly proportional to all other NMR signals. Therefore, quantitative measures of P species on a soil-weight basis were determined using solution ^{31}P NMR spectroscopy. The proportion of total P in NaOH-EDTA extracts as determined by NMR spectroscopy to that determined by ICP-OES, termed 'NMR observability' (Doolette, Smernik and Dougherty 2011), was on average 82% across all samples in the study.

DNA extraction, sequencing and quality control

Soil community DNA was extracted from 10 g of thawed soil of each treatment in triplicate using Mo Bio PowerSoil® DNA isolation kits (Mo Bio Laboratories, Inc. Carlsbad, CA, USA). DNA quantification and quality was assessed using a Qubit 2.0 fluorimeter (Thermo Fisher Scientific, Waltham, MA, USA) and 2100 Bioanalyzer DNA chips (Agilent Technologies, Santa Clara, USA). A total of 10 μg of high-quality DNA was provided for sequencing for each of the 18 samples.

Shotgun metagenomic sequencing of DNA was performed using 150 base paired-end chemistry on a BGISEQ-500 sequencing platform by BGI (Shenzhen, China). The generated raw sequences were limited to a minimum quality score of 25 and a minimum read length of 70 bases using TRIMMOMATIC (Bolger, Lohse and Usadel 2014). After filtering to remove substandard sequences, the average number of metagenome reads for each soil was 4.60 × 10^8 under maize—RockP, 4.57 × 10^8 under maize—TSP, 4.58 × 10^8 under maize—P0, 4.34 × 10^8 under sorghum—RockP, 4.33 × 10^8 under sorghum—TSP and 4.55 × 10^8 under sorghum—P0 (range across all datasets 3.83 × 10^8–4.62 × 10^8 reads).

Estimation of gene relative abundance and phylogeny

Each of the 18 metagenomes generated in this study were analyzed to assess the phylogenetic diversity of bacterial, archaeal and fungal small subunit ribosomal RNA genes and each of nine phosphohydrolase (PHO) genes using methods described by Neal

et al. (2017a,b). Nucleotide-based profile hidden Markov models (pHMMs) were generated from multi-sequence alignments (MSAs) of reference sequences of each gene using HMMBUILD, part of the HMMER suite version 3.1 (Eddy 2009). All MSAs were generated using the 1PAM/$\kappa = 2$ scoring matrix. For the 16S rRNA gene, pHMMs were generated from alignment of a set of 7245 bacterial and 266 archaeal 16S rRNA reference sequences associated with PAPRICA version 0.5.2 (Bowman and Ducklow 2015), built November 2019. For the fungal 18S rRNA gene, a pHMM was generated from 2447 reference sequences downloaded from the National Center for Biotechnology Information's Fungal 18S Ribosomal RNA RefSeq Targeted Loci Project, built February 2020. For phosphohydrolase genes, pHMMs were generated from 832 *phoD* sequences, 420 *phoX* sequences and 193 *phoA* alkaline phosphatase sequences, 107 β-propeller phytase (βPPhy) sequences, 101 cysteine phytase (CPhy) sequences and 226 histidine acid phytase (HAPhy) sequences described by Neal *et al.* (2017a), and for 457 class A, 319 class B and 457 class C non-specific acid phosphatase (NSAP) sequences described by Neal *et al.* (2017b). MSAs for all genes were generated using the *E-INS-i* iterative refinement algorithm in MAFFT version 7.3 (Katoh and Standley 2013). Metagenome reads with homology to each pHMM were identified using HMMSEARCH and a 1×10^{-5} expect-value (*E*) cutoff and a minimum bitscore of 37. To allow meaningful comparison between metagenomic datasets, PHO gene relative abundance was expressed as a proportion of the estimated total number of genomes in each dataset, assessed by estimating the abundance of the ubiquitous, single-copy genes *recA*, *gyrB* (Santos and Ochman 2004) and *atpD* (Gaunt *et al.* 2001). Nucleotide sequence-based pHMMs were developed for each gene as described in Neal *et al.* (2017a) using 1370 reference *recA* sequences, 2382 reference *gyrB* sequences and 1330 reference *atpD* sequences. Metagenome-derived homolog counts for each single-copy gene were size-normalized to the length of the shortest gene pHMM, *recA* accounting for differences in length between the genes. To do this, the pHMM length of *recA* (1164 nt) was divided by the pHMM length of the other single-copy genes (1392 nt for *atpD* and 2618 nt for *gyrB*), and this value was then multiplied by each single-copy gene count. The length-normalized abundance of each target phosphohydrolase gene was then calculated for each soil as [target gene count × read length/(mean normalized counts of single-copy genes)] (Howard *et al.* 2008).

PHMMER was used to compare the retrieved metagenome sequences, following six-frame translation using EMBOSS Transeq (Rice, Longden and Bleasby 2000), with the UniProtKB protein sequence database to confirm that the sequences represented the correct protein family. Only those metagenome sequences for which one of the six frame translations elicited a UniProtKB hit of the appropriate protein family ($E < 1 \times 10^{-5}$) was included in the subsequent analysis. Metagenome reads with confirmed homology to each gene were individually aligned to their respective full-length pHMM with HMMALIGN to generate an MSA. They were then assigned to branches of maximum-likelihood (ML) phylogenetic trees generated from the respective reference gene sets using RAxML version 8.2.4 (Stamatakis 2014). Phylogenetic placement was implemented using EPA-NG version 0.3.6 (Barbera *et al.* 2019) and visualized using iTOL version 5.5 (Letunic and Bork 2016). For the bacterial and archaeal 16S rRNA and fungal 18S rRNA genes, these placements can be translated into robust relative abundance estimates of organisms using the taxonomic labeling of the tree branches. This is not the case for PHO genes where instead placement indicates the degree of homology of metagenome reads (ecotypes) to the respective genes found in sequenced organisms, identified by taxonomic labels of the tree branches.

Phosphatase activity

The methods used for assaying the activities of phosphatase enzymes are described by Tabatabai (1994). The methods involve extraction and quantitative determination of μg *p*-nitrophenol released when soil is incubated with *p*-nitrophenyl phosphate or bis-*p*-nitrophenyl phosphate in modified universal buffer adjusted to pH 6.5 and 11 for acid and alkaline phosphatase, respectively. The reactions were stopped by adding $CaCl_2$ and NaOH, the solutions were centrifuged at 8000 rpm for 5 min and the supernatant was used for colorimetric measurements. Enzyme activities were assayed in triplicate rhizosphere soil samples.

Statistical analyses

To test our hypotheses, we generated gene assemblage-related metrics, including relative abundance, phylogenetic diversity (PD) and phylogeny-based distance metrics. The effects of different fertilizer treatments upon crop yield, phosphatase activity and estimates of gene normalized abundance and PD were analyzed using a nested analysis of variance (ANOVA) model after testing for homogeneity of variances using Levene's test and normality using the Shapiro–Wilk test. The model considered crop type (maize or sorghum) as the main factor with fertilization (RockP, TSP or P0) nested within crop type. Data for some genes were associated with significantly non-normal distributions, although the variances were homogenous. In these instances, permutation-based distribution-free tests of significance of *F*-values were adopted to calculate probability (denoted as p_{perm}). We calculated omega squared (ω^2) as an estimate of the extent to which variance in a response variable was accounted for by the treatment (effect size). Where significant treatment effects were identified, *post-hoc* pair-wise comparisons were performed using Tukey–Kramer Studentized Q, following the Copenhaver–Holland multiple comparison procedure (Holland and Copenhaver 1987) to control family-wise Type I error. All parametric tests were performed using PAST version 4.01 (Hammer, Harper and Ryan 2001). For all tests, an α of 0.05 was considered significant.

Estimates of gene phylogenetic (that is, sequence similarity-sensitive) diversity based upon placement of homologous metagenomic reads were assessed by computing a measure incorporating abundance, using the FPD binary in GUPPY version 1.1 (part of the PPLACER code, Matsen, Kodner and Armbrust 2010) accounting for reference ML tree pendant branch length. The measure equates Faith's PD (McCoy and Matsen 2013). To assess the depth of sequencing of the soil communities compared with the total diversity of the PHO genes within them, rarefaction curves of expected mean phylogenetic diversity (Nipperess and Matsen 2013) were generated using the GUPPY RAREFACT binary, interpreting placement weights as counts and calculating up to a rarefaction size (*k*) of 70 000. Additionally, unconstrained ordination based upon principal component analysis of the difference in placement densities on reference tree branches—termed edge-PCA (Matsen and Evans 2013)—was used for graphical representation of phylogeny-based differences between treatments in a 2D plane using the EDGEPCA binary in the GAPPA code version 0.4.0 (Czech and Stamatakis 2019), treating each query as a point mass concentrated on the highest weight placement. An advantage of edge-PCA is that

branches associated with placements contributing to eigenvalues on each axis are identified and for 16S and 18S rRNA gene analysis, organisms contributing to the observed differences can be identified. This is not the case for PHO genes where only association with sequenced homologs can be identified.

To assess 16S rRNA, 18S rRNA and PHO gene-based β-diversity between the different crops and fertilizer treatments, Kantorovich–Rubinstein (KR) phylogenetic distance metrics (Evans and Matsen 2012) were calculated from phylogenetic placements of metagenome reads using the GAPPA KRD binary, treating each query as a point mass concentrated on the highest weight placement. The KR distance metric, which is allied to the weighted-UniFrac measure (Evans and Matsen 2012), compares gene assemblage distributions on a phylogenetic tree in units of nucleotide substitutions per site, a biologically meaningful approach to comparing communities. Differences in gene assemblages based upon KR metrics were tested using permutational multivariate analysis of variance (PERMANOVA; Anderson and ter Braak 2003) following testing for homogeneity of multivariate dispersions among *a priori* groups using PERMDISP (permutational test of homogeneity of multivariate dispersion; Anderson 2006). The same nested model was adopted for PERMANOVA as described above for ANOVA and significance was based upon 99 999 permutations. Multivariate tests were performed using PRIMER PERMANOVA+ version 7.0.13 (PRIMER-e, Auckland, New Zealand).

RESULTS

Crop performance

Maize and sorghum were grown in 2018/2019, the second year of P fertilization regimes with TSP and RockP. For maize, there was no statistically significant effect of P fertilization ($F_{2,6} = 2.2$, $p = 0.197$, $\omega^2 = 0.204$) on yield: a mean yield of 9.64 $\pm$ 0.41 Mg ha^{-1} was achieved across all treatments. A significant effect of P fertilization was observed for sorghum yields ($F_{2,6} = 9.0$, $p = 0.016$, $\omega^2 = 0.639$). In this case, TSP fertilization (yield, 3.97 $\pm$ 0.19 Mg ha^{-1}) resulted in a significantly greater yield than unfertilized soil (P0 yield, 3.38 $\pm$ 0.04 Mg ha^{-1}, Q = 5.9, $p = 0.014$). Fertilization with RockP resulted in a mean yield of 3.60 $\pm$ 0.12 Mg ha^{-1}, not significantly different from either of the other two treatments.

Soil phosphorus

Concentrations of total NaOH-EDTA extractable P ranged from 277 to 547 mg-P kg^{-1} soil, of which 60–85% was comprised of inorganic P (Table 1). The fertilized treatments generally have concentrations of extractable soil P that are greater than the P0 treatment, except for that of the RockP treatment under sorghum that was slightly lower than P0. Concentrations of extractable inorganic P were generally higher under maize than sorghum, and under TSP compared with P0. Concentrations of organic P ranged from 81 to 109 mg-P kg^{-1} soil, which accounted for 15–40% of total extractable P. Concentrations of extractable organic P were generally similar among treatments, but slightly lower under RockP compared with P0 and TSP.

Solution 31P NMR spectra on soil extracts were highly resolved and revealed a plethora of organic P species (Fig. 1). The majority of NMR signal (>95%) was in the orthophosphate and phosphomonoester regions. The identifiable sharp peaks in these regions, shown in Fig. 1, included: (i) orthophosphate (δ 5.38 ppm); (ii) *scyllo*-IP6 (δ 3.26 ppm); (iii) four peaks due to *myo*-IP6 (δ 5.06, 4.11, 3.73 and 3.62 ppm); (iv) *neo*-IP6 in the 4-equatorial/2-axial position (δ 5.95 and 3.78 ppm); (v) three peaks due to D-*chiro*-IP6 in the 2-equatorial/4-axial position (δ 5.70, 4.30 and 3.88 ppm); (vi) *scyllo*-IP5 (δ 3.89, 3.33 and 3.15 ppm); (vii) *myo*-IP5 of the (1,2,4,5,6) enantiomer (δ 4.52, 4.01, 3.73, 3.42 and 3.31 ppm); (viii) *myo*-IP5 of the (1,3,4,5,6) enantiomer (δ 4.21, 3.62 and 3.31 ppm); and (ix) *scyllo*-IP4 (δ 4.30 ppm). In addition, there was an underlying 'broad' signal centered at δ 4.10 ppm with a linewidth of 300 Hz. A comparison of ^{31}P NMR spectra is presented in Fig. 2 and demonstrates a complex but consistent P chemistry in the soil where both crops were cultivated under the contrasting fertilization regimes.

Quantification of the various P moieties is presented in Table 1. Phosphomonoesters comprised on average 97% of the extractable organic P across the analyzed soil. The broad signal (on average 52%) and inositol phosphates (on average 34%) were the predominant pools of phosphomonoesters. Concentrations of the broad signal were generally similar among treatments, but lower under RockP compared with P0 and TSP. Concentrations of IP_6 and lower order inositol phosphates (i.e. IP_5 and IP_4) comprised on average 24% and 10% of the total pool of phosphomonoesters and were generally unchanged among the treatments.

Phosphatase activity

Sorghum rhizosphere soil supported greater phosphatase activity at both pH 6.5 and 11 (188.0 $\pm$ 16.1 and 83.7 $\pm$ 11.1 Units L^{-1}, respectively) than maize rhizosphere soil (150.0 $\pm$ 27.3 and 49.0 $\pm$ 12.6 Units L^{-1}, respectively). However, the overall effect of crop species upon phosphatase activity at either alkaline ($F_{1,12} = 1.8$, $p = 0.200$) or acid ($F_{1,12} = 0.52$, $p = 0.483$) pH was not significant. Significant effects were observed for the different fertilizer applications—nested within crop species—at both alkaline ($F_{4,12} = 4.2$, $p = 0.024$, $\omega^2 = 0.328$) and acid ($F_{1,12} = 6.5$, $p = 0.005$, $\omega^2 = 0.484$) pH. The effect size associated with fertilization was greater under acid conditions. In both cases, phosphatase activity was greatest in P0 soils and least in soils amended with RockP (Fig. 3).

Small subunit ribosomal RNA-based community analysis

Bacterial communities in all soils were dominated (collectively representing >30% of all reads) by the Acidobacteria *Luteitalea pratensis*, *Candidatus* Solibacter usitatus, *Chloracidobacterium thermophilum* and *Ca*. Koribacter versatilis; the Actinobacteria *Conexibacter woesei* and *Baekduia soli*; the Gemmatimonadete *Gemmatirosa kalamazoonesis*; Proteobacteria including the α-Proteobacteria *Rhodoplanes* sp. Z2-YC6860 and *Sphingomonas ginsengisoli*, the β-Proteobacteria bacterium GR16–43 and the δ-Proteobacterium *Haliangium ochraceum*; the Verrucomicrobium *Ca*. Xiphinematobacter sp.; and the Terribacterium group organism *Thermobaculum terrenum*. Dominant Archaea included the Lokiarcheote *Ca*. Prometheoarchaeum syntrophicum MK-D1, the Crenarchaeotes *Ca*. Mancarchaeum acidiphilum MIA14, *Ca*. Korarchaeum cryptofilum OPF8, *Desulfurococcus amylolyticus* and *Pyrobaculum arsenaticum*, and the Euryarchaote Methanomicrobia *Methanothrix soehngenii* and *Methanosaeta harundinacea*. Fungal communities were dominated by the Dothidiomycetes *Brunneoclavispora bambusae* and *Recurvomyces mirabilis*; the Saccharomycete *Starmerella ratchasimensis*; the Mucormycete *Gongronella orasabula*; the Entomophthoromycete *Conidiobolus obscurus*; the Sordariomycetes *Cornuvesica acuminata*, *Dactylidispora singaporensis* and *D. ellipsospora*;

Table 1. Concentrations (mg kg^{-1}) of phosphorus (P) species in NaOH-EDTA extracts of one replicate of the three fertilizer treatments under continuous cropping from sorghum or maize as determined from solution ^{31}P NMR spectroscopy. Rock phosphorus (RockP) and triple superphosphate (TSP) treatments were associated with the addition of 100 kg of fertilizer ha^{-1} yr^{-1}. No phosphorus was added to the control treatment (P0).

	Sorghum			Maize		
P species	P0	RockP	TSP	P0	RockP	TSP
Phosphonates						
2-AEP	0.0	0.6	0.7	0.5	0.0	0.6
Other[a]	0.0	0.0	0.0	0.0	0.0	0.4
Orthophosphate	159.5	174.6	274.6	219.6	463.2	344.7
Phosphomonoester						
Broad signal	54.3	34.1	63.2	55.3	37.0	55.1
myo-IP6	19.0	16.5	17.9	16.8	19.5	20.9
scyllo-IP6	3.4	2.1	1.9	1.5	2.0	2.0
neo-IP6	1.5	0.7	0.0	0.0	0.0	0.0
D-*chiro*-IP6	0.0	1.6	0.0	1.5	2.6	2.1
myo-IP5[b]	6.6	8.5	9.9	8.0	7.2	9.7
scyllo-IP5	1.7	1.8	0.0	0.8	1.0	1.2
scyllo-IP4	0.8	0.0	0.0	0.5	0.0	0.0
Other[a]	16.2	20.5	9.9	9.0	11.7	10.3
Phosphodiester						
DNA	5.6	0.0	4.8	3.6	0.0	0.0
Other[a]	0.5	0.0	0.0	0.0	0.0	0.0
Polyphosphate						
Pyrophosphate	8.0	3.0	7.6	3.9	2.6	2.8
Other[a]	0.0	0.0	0.0	0.3	0.0	0.0
Total P	276.9	263.9	390.6	321.3	547.2	449.8
Inorganic P	167.5	177.6	282.2	223.8	465.8	347.5
Organic P	109.4	86.3	108.3	97.5	81.4	102.3

[a]Summation of all sharp signals of unknown identity within the phosphonate, phosphomonoester, phosphodiester or polyphosphate regions.
[b]Summation of *myo*-IP5 of the (1,2,4,5,6) and (1,3,4,5,6) enantiomers.

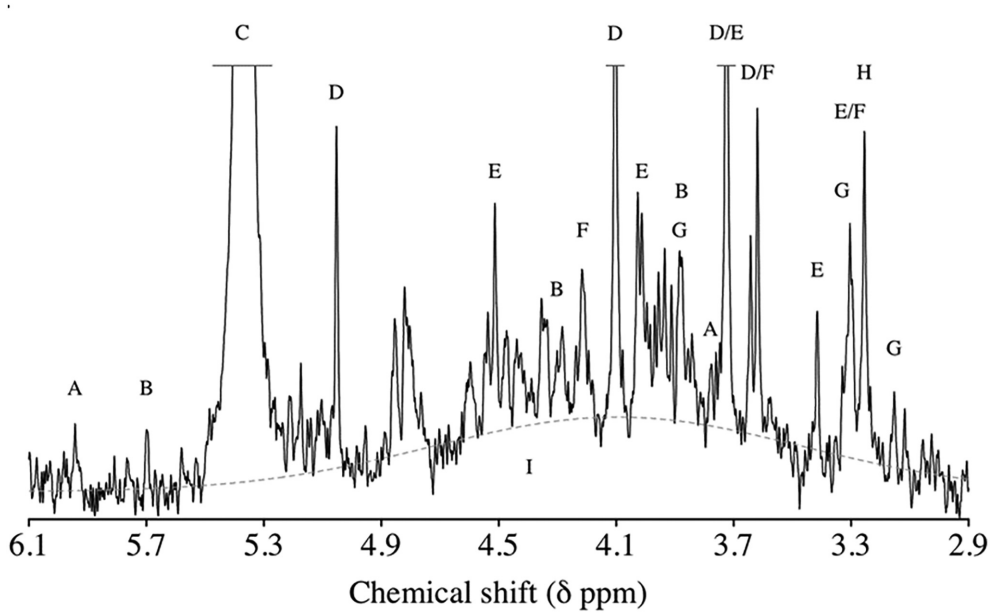

Figure 1. A solution phosphorus-31 NMR spectrum of the orthophosphate and phosphomonoester regions (δ 6.1 to 2.9 ppm) generated from a soil extract. Phosphorus species that have been identified within this region include: A—*neo*-IP6 in the 4-equatorial/2-axial conformation (δ 5.94 and 3.78 ppm), B—D-*chiro*-IP6 in the 2-equatorial/4-axial conformation (δ 5.70, 4.30 and 3.88 ppm), C—orthophosphate (δ 5.37 ppm), D—*myo*-IP6 (δ 5.05, 4.10, 3.72 and 3.62 ppm), E—*myo*-IP5 of the (1,2,4,5,6) enantiomers (δ 4.51, 4.01, 3.72, 3.42 and 3.30 ppm), F—*myo*-IP5 of the (1,3,4,5,6) enantiomers (δ 4.21, 3.62 and 3.30 ppm), G—*scyllo*-IP5 (δ 3.88, 3.33 and 3.15 ppm), H—*scyllo*-IP6 (δ 3.26 ppm) and I—a broad signal (centered around δ 4.10 ppm with a linewidth of 300 Hz).

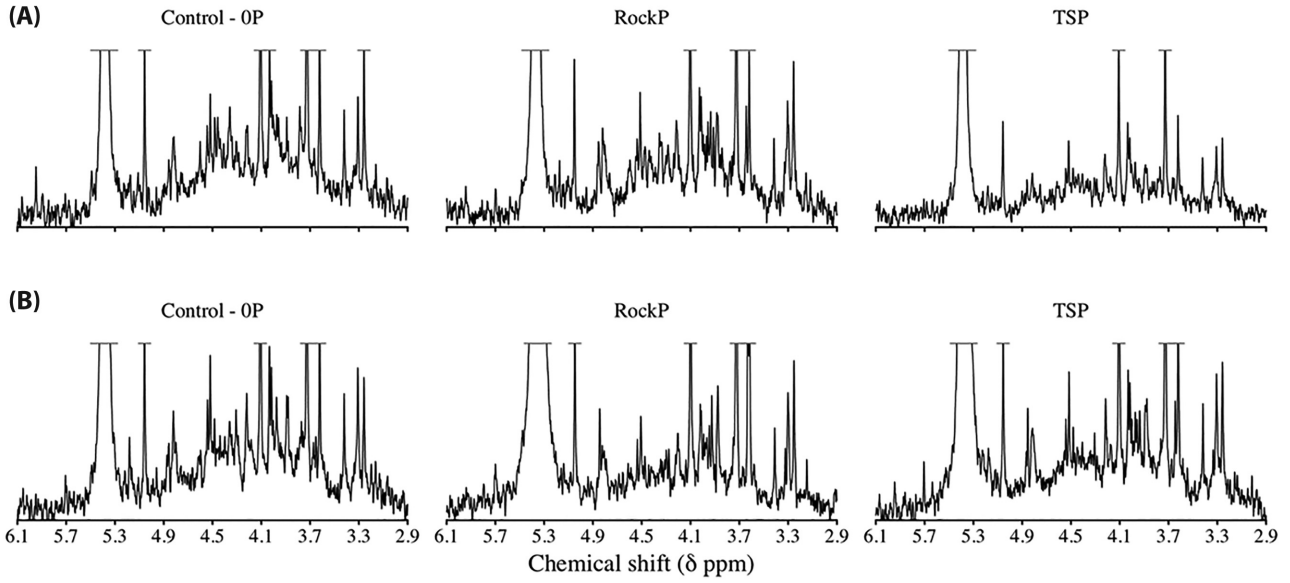

Figure 2. Solution phosphorus-31 NMR spectra of the orthophosphate and phosphomonoester regions (δ 6.1 to 2.9 ppm) on extracts from soils of the long-term field experiment in Sete Lagoas, Brazil. Cropping treatments include continuous cultivation with sorghum **(A)** or maize **(B)**. Fertilizer treatments include no addition of fertilizer P (Control—P0), the addition of rock phosphate at a rate of 100 kg fertilizer ha^{-1} yr^{-1} (RockP) or the addition of triple superphosphate at a rate of 100 kg fertilizer ha^{-1} yr^{-1} (TSP).

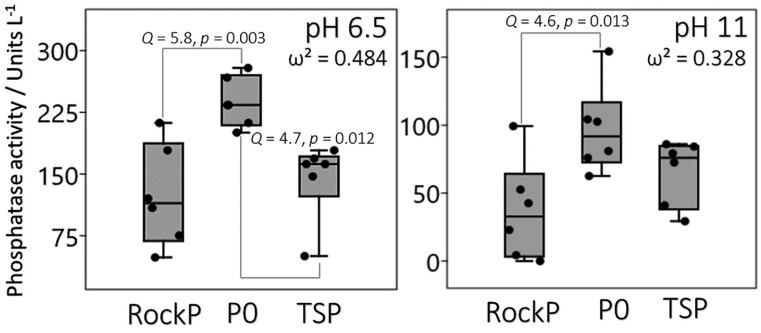

Figure 3. Phosphatase activity measured in soil collected from rhizospheres of maize and sorghum plants fertilized with either RockP or triple superphosphate fertilizer (TSP), compared with activity in unfertilized soil (P0). There was no significant effect of crop type upon enzyme activity. The effect size (ω^2) of fertilization upon phosphatase activity was greater under acidic conditions. Studentized Tukey–Kramer *post-hoc* pair-wise comparisons (Q) of enzyme activity are shown. Box plots show the interpolated 25% and 75% quartiles with the median represented as a horizontal line. Whiskers indicate the minimum and maximum values. Enzyme activity was assessed by estimating the hydrolysis of disodium-*p*-nitrophenyl phosphate in buffered solutions.

the Umbelopsidomycete *Umbelopsis changbaiensis*; and the Kickxellomycete *Coemansia umbellata*.

Fungal community phylogenetic diversity was largely stable across the experiment (Fig. 4). There was a significant effect of crop type ($F_{1,12} = 16.8$, $p = 0.001$) upon bacterial PD. The maize rhizosphere supported greater PD (10 046 ± 174) than the sorghum rhizosphere (8935 ± 228), but there was no significant effect of fertilization ($F_{4,12} = 0.86$, $p = 0.514$). A similar trend was observed for archaea: maize supported significantly ($F_{1,12} = 10.7$, $p = 0.007$) higher archaeal PD (77 932 ± 1199) than sorghum (70 805 ± 1961), with no significant effect of fertilization ($F_{4,12} = 0.87$, $p = 0.508$). The effect size associated with crop type was larger for bacteria than archaea. For fungi, there was no significant effect of either crop type ($F_{1,12} = 3.9$, $p = 0.071$) or fertilization ($F_{4,12} = 0.51$, $p = 0.732$) upon 18S rRNA-based PD.

There were no statistically significant differences in either bacterial (PERMANOVA, *pseudo*-$F_{4,12} = 0.62$, $p_{perm} = 0.620$) or archaeal (*pseudo*-$F_{4,12} = 0.51$, $p_{perm} = 0.985$) 16S rRNA- or 18S rRNA-based (*pseudo*-$F_{4,12} = 0.63$, $p_{perm} = 0.862$) community phylogenetic assemblages (β-diversity) due to fertilization, assessed using KR distance determined from placement of homologous reads on the respective phylogenetic trees.

Bacterial 16S rRNA-based (*pseudo*-$F_{1,12} = 1.7$, $p_{perm} = 0.127$) and fungal 18SrRNA-based (*pseudo*-$F_{1,12} = 1.6$, $p_{perm} = 0.178$) assemblages were also not affected by crop type. However, crop type did influence archaeal 16S rRNA-based (*pseudo*-$F_{1,12} = 2.1$, $p_{perm} = 0.042$) assemblages.

To investigate the likely source of these archaeal assemblage differences identified by PERMANOVA of KR distance metrics, we used a multivariate ordination procedure, edge-PCA, which exploits the phylogenetic structure inherent in the data. Edge-PCA analysis of the archaeal 16S rRNA homologs indicated several species that were sensitive to crop type (Fig. 5). Differences were associated with edge-PCA axis 2, which accounted for ~20% of total variability. This indicated that Haloarchaea such as *Natronobacterium gregoryi* together with Methanobacteria

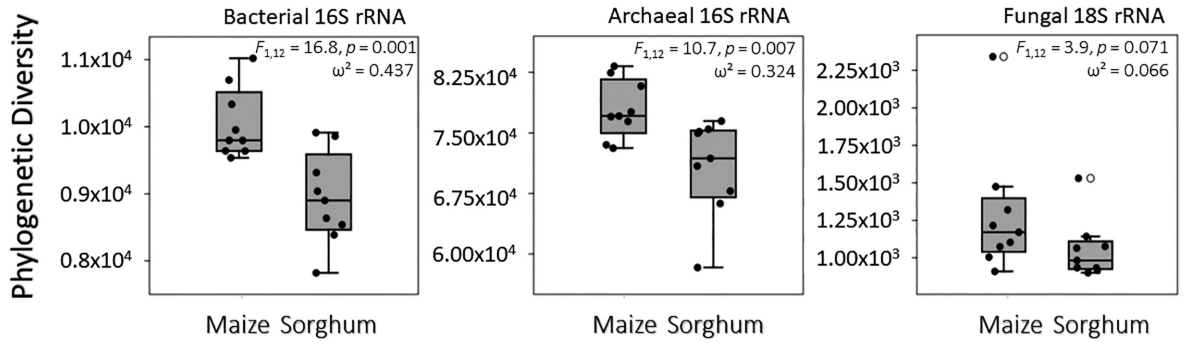

Figure 4. The PD—defined as the sum of branch lengths of the respective reference phylograms associated with metagenome reads—of small subunit ribosomal RNA marker genes identified in rhizospheres of maize and sorghum grown in Cerrado soil. There was no significant effect of phosphorus fertilization upon PD. For each marker gene, results of ANOVA and effect size estimates (ω^2) are given. Box plots indicate the interpolated 25% and 75% quartiles with the median represented as a horizontal line. Whiskers indicate minimum and maximum values. Where necessary, outliers are identified with open circles; in this case, whiskers are drawn from the limits of the upper and lower quartiles to data points <1.5 times the interquartile range.

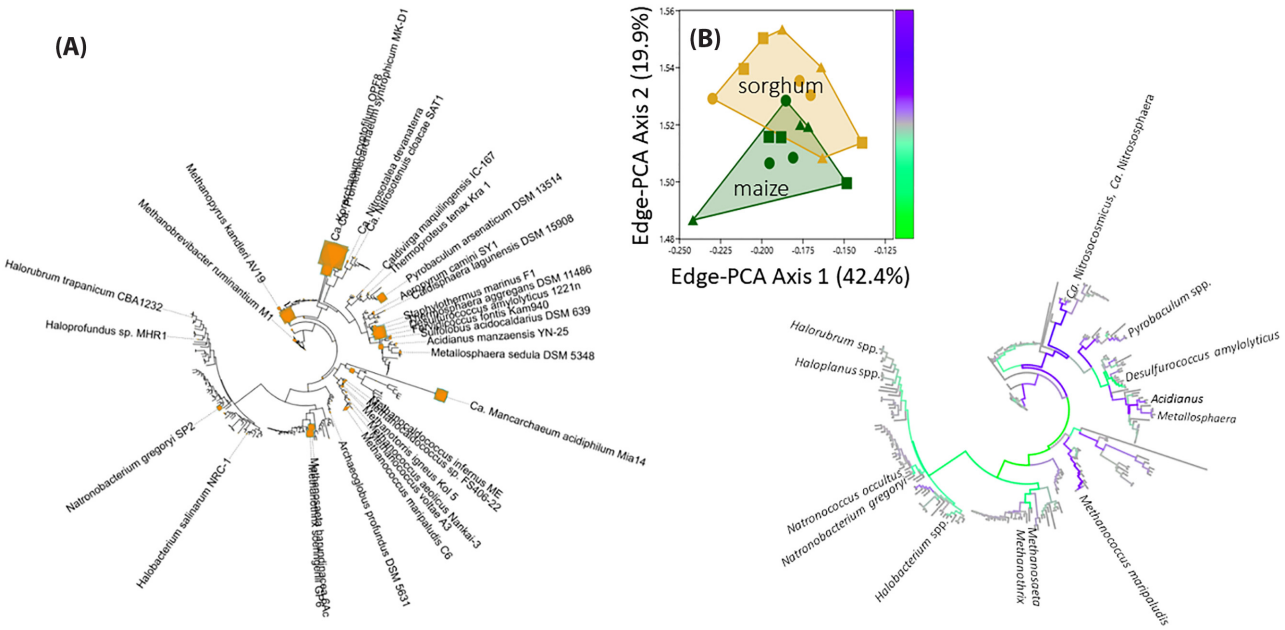

Figure 5. Phylogenetic comparison of Archaeal species assemblages in rhizospheres of maize (green placements and data points) and sorghum (yellow placements and data points) grown in Cerrado soil. **(A)** Overall phylogenetic placement of metagenome reads with homology to the archaeal 16S rRNA gene in soils receiving RockP (indicated with circular placements and data points), TSP (indicated with square placements and data points) or no phosphorus fertilization (P0—indicated with triangle placements and data points). The most abundant organisms are identified by taxonomic name on branch tips of the maximum-likelihood archaeal reference 16S rRNA phylogram. Placement symbol size is scaled to reflect relative abundance across the 18 samples. **(B)** Ordination of archaeal 16S rRNA assemblages shown in (A), exploiting the underlying phylogenetic nucleotide sequence structure (edge-PCA). Gene assemblages associated with maize and sorghum are separated on edge-PCA axis 2. Edges associated with large eigenvectors are shown in the associated color-coded phylogram, and organisms related to each branch are identified by taxonomic name. Branch color corresponds to edge-PCA axis 2 color scale. The arrow associates the color-coded phylogram with its corresponding edge-PCA axis.

Methanosaeta and *Methanothrix*, as well as *Desulfurococcus amylolyticus* were more associated with maize rhizospheres. The Nitrososphaeraceae *Ca*. Nitrososphaera and *Ca*. Nitrosocosmicus, *Methanococcus maripaludis*, and the Crenarchaeotes *Pyrobaculum*, *Acidianus* and *Metallosphaera* were all more associated with sorghum rhizospheres.

Phosphohydrolase gene abundance and phylogenetic diversity

Comparison of phylogenetic rarefaction curves (Figure S1, Supporting Information) indicated that all PHO genes were undersampled with respect to the total biodiversity in the soils. However, differences in sampling effort between the different treatments were limited and so direct comparisons were performed without resorting to rarefaction of the sequence data, which increases both Type I and II statistical errors (McMurdie and Holmes 2014). These rarefaction curves also demonstrate the relative phylogenetic diversity and abundance between the alkaline phosphatases *phoD* and *phoX*, class A and C non-specific acid phosphatases and the β-propeller phytase genes in the soils. Genes of *phoD* were both the most numerous and phylogenetically diverse of the genes, but *phoX* and the two NSAPs were all similarly numerous and diverse. We assessed phosphohydrolase gene abundance by normalizing counts with respect to the length-adjusted counts of three single-copy marker genes; *atpD*, *recA* and *gyrB*. Using this approach, alkaline phosphatase *phoD* and *phoX*, NSAP class A

and the βPPhy gene normalized abundances were shown to be different between plant species, all having significantly greater normalized abundance in sorghum rhizospheres than those of maize (Fig. 6), contrary to the limited effects of crop type upon overall community assemblages. Fertilization had no significant influence upon the normalized abundance of any PHO gene. PD of *phoD*, class C NSAPs and βPPhy genes was also sensitive to crop type with sorghum associated with higher PD (Fig. 6). There was no significant effect of fertilization upon PHO PD. The phylogenetic placements of PHO genes showing sensitivity to crop type are shown, respectively, in Figs 7 and 8 for the alkaline phosphatases *phoD* and *phoX*, Figs 9 and 10 for class A and C NSAPs, and Fig. 11 for the β-propeller phytase gene.

KR distance-based assessment of the sensitivity of ecotype assemblages of each PHO gene to crop type and soil fertilization indicated that significant differences in assemblage phylogeny were apparent for all genes except the three phytase families. This indicates a consistent phytase assemblage in all soils considered in this experiment. For the alkaline and non-specific acid phosphatase genes, PERMANOVA identified significant differences in assemblage in response to crop type (smallest *pseudo*-$F_{1,12} = 2.0$, $p_{perm} = 0.016$, *phoX*), but not fertilization. Heterogeneity of multivariate dispersion was only detected for the alkaline phosphatase *phoA* (PERMDISP, *pseudo*-$F_{1,2} = 8.9$, $p_{perm} = 0.009$), where ecotype assemblages showed reduced heterogeneity in sorghum rhizospheres compared with maize.

For the alkaline phosphatases *phoD* and *phoX* and the two NSAPs for which differences in assemblages due to crop type were observed, we investigated the ecotypes responsible for these differences. For *phoD*, the first two edge-PCA axes accounted for 76% of total phylogenetic variation, separating crops largely on the first axis (Fig. 7). The analysis identified ecotypes with homology to *phoD* genes of a clade of closely related α-proteobacteria *Sphingopyxis* sp., *Asticcacaulis* sp. and β-proteobacteria *Ralstonia* sp. and *Cupriavidus* sp., a second closely related clade comprised of the β-proteobacteria *Rhodoferax ferrireducens* and *Polaromonas* sp. CF318 and a separate clade comprised of the Gemmatimonadetes *Gemmatirosa kalamazoonesis* and *Gemmatimonas* spp. as being more associated with sorghum; and ecotypes with homology to *phoD* genes of a clade of the Actinobacteria *Nocardioides*, *Arthrobacter* and *Streptomyces*, and the γ-proteobacterium *Salinisphaera shabensis* as being more associated with maize. Ecotypes of the alkaline phosphatase *phoX* (Fig. 8) identified as contributing to differences between crop type were again largely associated with edge-PCA axis 1 (accounting for 53% of total variability), but there was a less clear distinction than for *phoD*. In this case, ecotypes with homology to *phoX* gene sequences of the α-proteobacterium *Agrobacterium* sp., the β-proteobacteria *Variovorax paradoxus* B4 and unclassified Methylophilaceae bacterium 11, as well as the γ-proteobacterium *Pseudomonas syringae*, were more associated with sorghum, while ecotypes showing homology to a closely related clade comprised of the β-proteobacterium *Ramlibacter tatouinensis* and the α-proteobacteria *Novosphingobium* sp. and *Asticcacaulis* sp. and the more distantly related *Pseudomonas stutzeri* were all associated more with maize. Class A NSAP ecotypes showed the greatest separation between crop type on edge-PCA axis 1 (Fig. 9) of all the four PHO genes studied in detail. Combined, the first two axes accounted for 74% of NSAPa phylogenetic variation. Ecotypes sensitive to crop type were dominated by proteobacteria, including those with homology to a large clade of the α-proteobacterium *Bosea* spp. and the β-proteobacterium *Achromobacter* spp. associated more with maize and a more phylogenetically diverse group of ecotypes including the α-proteobacterium *Caulobacter* spp., and the β-proteobacteria *Burkholderia* sp. H160 and *B. fungorum*, *Collimonas* sp. and *Herbaspirillum rubrisubalbicans*, all more associated with sorghum. Ecotypes of class C NSAP associating with sorghum also showed homology to genes of the α-proteobacterium *Thioclava* spp. and the γ-proteobacteria *Xanthomonas* spp. and *Stenotrophomonas* spp. (Fig. 10). In contrast, ecotypes associating with maize showed homology to genes associated Bacteroidetes, including a clade comprised of *Pedobacter* sp. BMA and *Capnocytophaga* sp. and *Flavobacterium* sp. Leaf 82. The first edge-PCA axis accounted for 52% of the total NSAPc phylogenetic variation. Edge-PCA did not identify any clear separation of crop type despite a significant difference in ecotype assemblage.

DISCUSSION

The use of rock phosphates for crop production in acidic, highly weathered tropical soils such as those found in large regions of South America, Africa and Australia can be a cost-effective alternative to highly processed phosphate fertilizers (TSP). This is because RockP is less reactive than TSP and dissolves slowly once applied to acidic soils, minimizing the rapid complexation of P by iron and aluminum oxides. Consequently, the use of RockP in place of TSP may shift P utilization of crops within agricultural systems toward P made bioavailable by the activities of phosphohydrolase enzymes acting on organic P. However, there is little information regarding the effect of P fertilization upon microbial communities associating with important crops in these soils, or the diversity of genes coding for phosphohydrolase enzymes in crop rhizospheres. To address these issues, we studied the performance and response of two economically important crops, maize and sorghum, to phosphorus fertilization, generating information regarding the speciation of extractable P and activity of phosphatase enzymes in rhizosphere soils.

Crop yields were similar when fertilized with RockP or TSP, which is consistent with previous observations in Cerrado soils (Silva *et al.* 2017). This demonstrates that RockP can be an effective source of fertilizer P for crops in Cerrado soils and can contribute to a reduction in the amount of phosphate fertilizers applied annually. Phosphatase activity was the only biological parameter that we observed to be influenced by P fertilization. Enzyme activity was significantly higher in the absence of fertilization (P0) than in fertilized soil at both acid and alkaline pH, but activities were similar under RockP and TSP fertilization (Fig. 3). The reduced phosphatase activity may be related with a structural remodeling of rhizosphere microbial populations that may require longer to become metabolically active after P-source addition. There was no association between phosphatase activity and the abundance or phylogenetic diversity of genes predicted to code for these enzymes. Despite RockP and TSP having similar effectiveness in supporting crop yields, the accumulation of fertilizer P into pools of organic soil P differed between the two fertilized treatments. Slightly lower concentrations of soil organic P under the RockP treatment compared with the P0 and TSP treatments may be due to the 'liming' effect of RockP on soil pH and net P addition (Loganathan *et al.* 2005; Margenot *et al.* 2016). The results of a sixteen-year field study showed that continuous use of certain phosphate rocks can slow down the rate of acidification significantly in pasture soils (Loganathan *et al.* 2005). However, the RockP 'liming' effect was not sufficient to increase alkaline phosphatase activity. The relatively more alkaline soil pH due to the addition of RockP may have improved

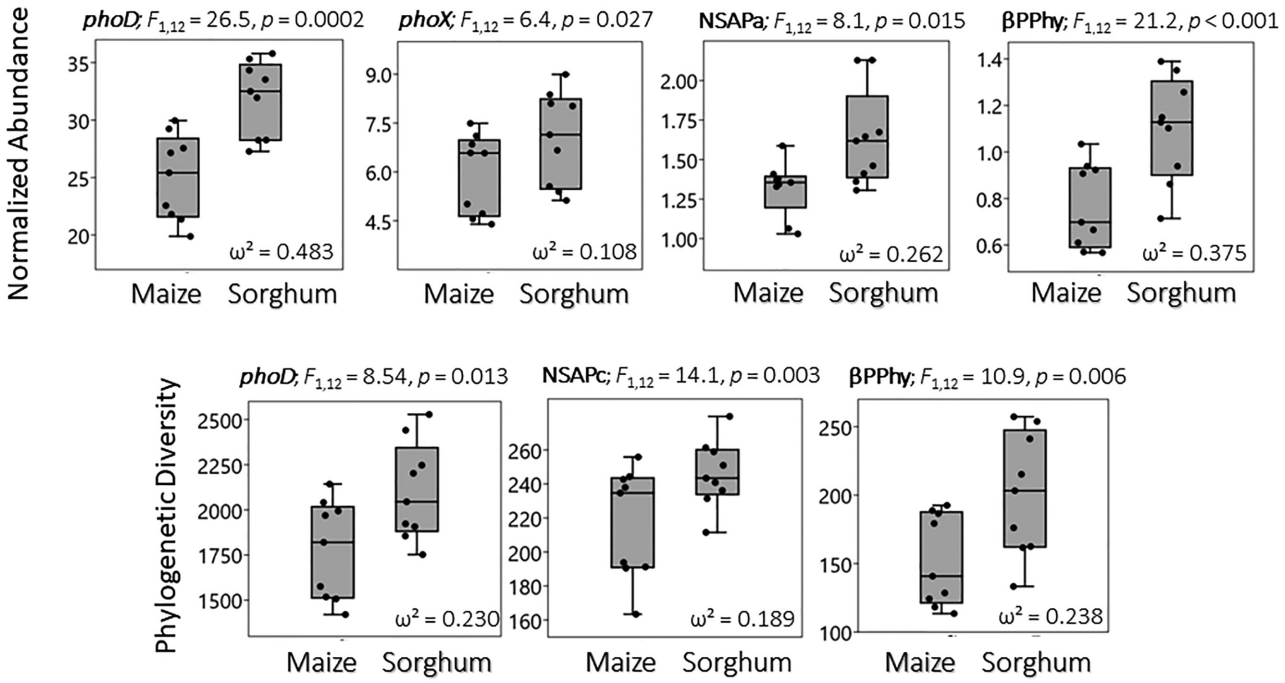

Figure 6. Abundance and PD (defined as the sum of branch lengths of the respective reference phylograms associated with metagenome reads) of phosphohydrolase genes in rhizosphere soil of maize and sorghum. No significant effect of phosphorus fertilization upon gene abundance or PD was observed. Only comparisons for which a significant effect of crop type were detected are shown. Length-normalized abundance (relative to the abundance of *atpD*, *gyrB* and *recA* single-copy genes, see the 'Materials and Methods' section for calculation) and PD of gene ecotypes were consistently higher in sorghum rhizospheres where significant differences were identified by ANOVA. For each gene, results of ANOVA and effect size estimates (ω^2) are given. Box plots indicate the interpolated 25% and 75% quartiles with the median represented as a horizontal line. Whiskers indicate minimum and maximum values.

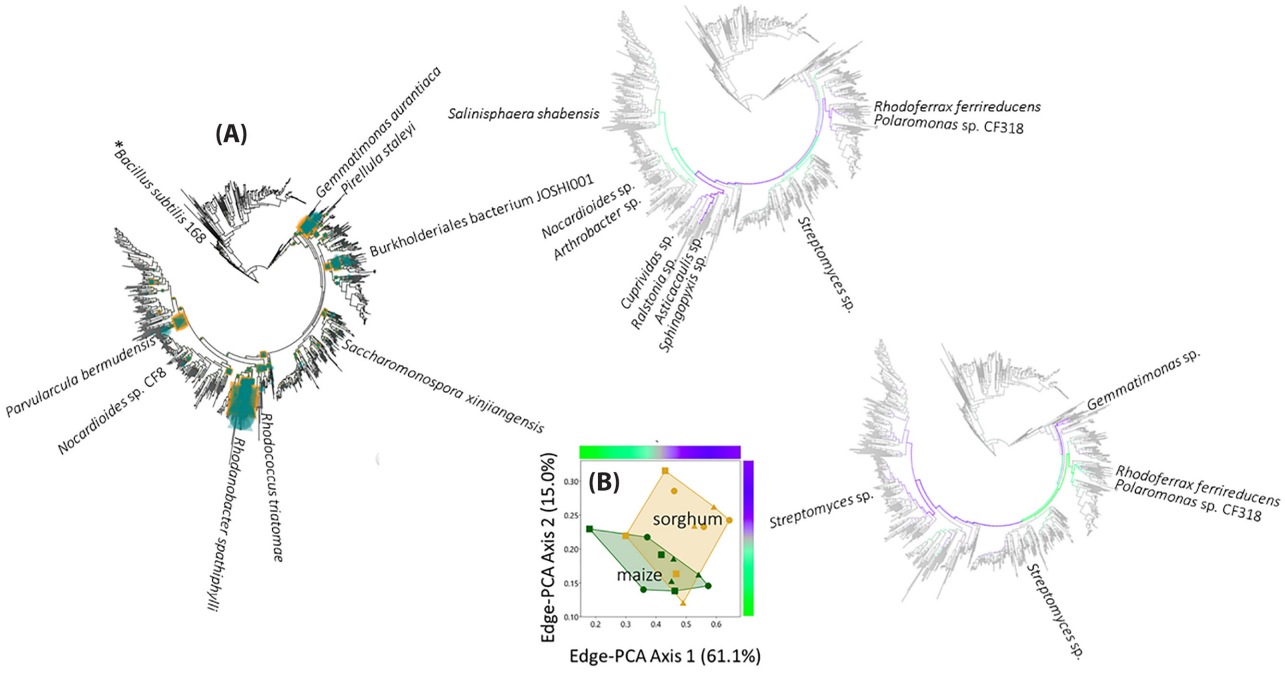

Figure 7. Phylogenetic comparison of alkaline phosphatase gene *phoD* ecotype assemblages in rhizospheres of maize (green placements and data points) and sorghum (yellow placements and data points) grown in Cerrado soil. **(A)** Phylogenetic placement of metagenome reads with homology to the *phoD* gene in soils receiving RockP (indicated with circular placements and data points), TSP (indicated with square placements and data points) or no phosphorus fertilization (P0—indicated with triangle placements and data points). The most abundant organisms are identified by taxonomic name on branch tips of the maximum-likelihood archaeal reference 16S rRNA phylogram. Placement symbol size is scaled to reflect relative abundance across the 18 samples. Asterisk (*) indicates the SWISS-PROT phoD accession. **(B)** Ordination of *phoD* assemblages shown in (A), exploiting the underlying phylogenetic nucleotide sequence structure (edge-PCA). Edges associated with large eigenvectors are shown in the associated color-coded phylograms, and organisms related to each branch are identified by taxonomic name. Branch color corresponds to edge-PCA axis color scales. The arrow associates each color-coded phylogram with its corresponding edge-PCA axis. Gene assemblages associated with maize and sorghum are separated across both edge-PCA axes.

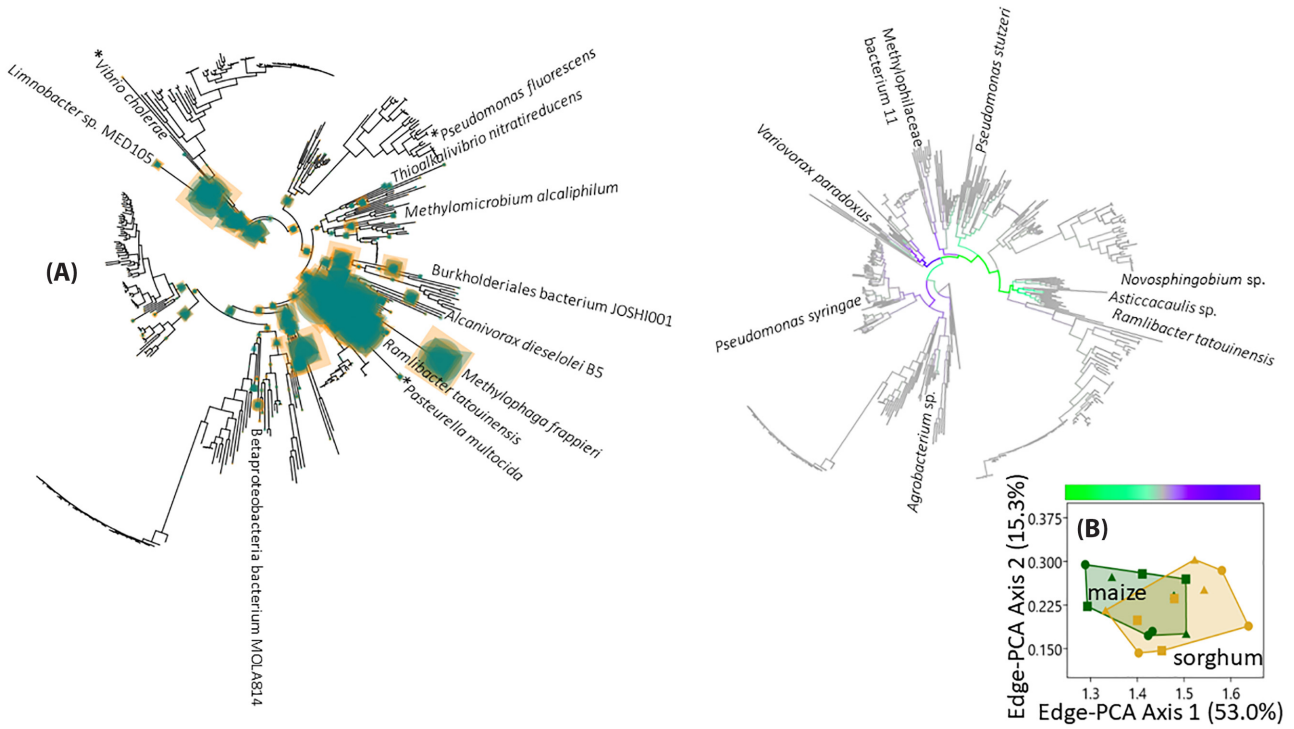

Figure 8. Phylogenetic comparison of alkaline phosphatase *phoX* ecotype assemblages in rhizospheres of maize (green placements and data points) and sorghum (yellow placements and data points) grown in Cerrado soil. **(A)** Phylogenetic placement of metagenome reads with homology to reference *phoX* genes in soils receiving RockP (indicated with circular placements and data points), TSP (indicated with square placements and data points) or no phosphorus fertilization (P0—indicated with triangle placements and data points). Organisms harboring the *phoX* genes with which ecotypes share homology are identified on branch tips of the maximum-likelihood *phoX* reference phylogram. Placement symbol size is scaled to reflect relative abundance across the 18 samples. Asterisk (*) identifies *phoX* genes described by Majumdar, Ghatak and Ghosh (2005), Wu *et al.* (2006) and Monds *et al.* (2006). **(B)** Ordination of *phoX* assemblages shown in (A), exploiting the underlying phylogenetic nucleotide sequence structure (edge-PCA). Edges associated with large eigenvectors are shown in the associated color-coded phylogram, and organisms related to each branch are identified by taxonomic name. Branch color corresponds to the edge-PCA axis color scale. The arrow associates the color-coded phylogram with its corresponding edge-PCA axis. Gene assemblages associated with maize and sorghum are separated on edge-PCA axis 1.

microbial activity and the mobilization of soil organic P. Complex forms of organic P (as a broad NMR signal) were the predominant pool of soil organic P that decreased under the RockP treatment compared with P0 and TSP. This pool of organic P is associated with P in large supra-macromolecular structures as part of the soil organic matter. Consequently, the mobilization or P within soil organic matter may be an important source of P in these soils when P is limiting crop growth.

A diverse range of inositol phosphates, including lower order inositol phosphates (i.e. IP_5 and IP_4), were detected in these soils, comprising about one-third of the total pool of organic P. Since concentrations of inositol phosphates remained unchanged among treatments, their bioavailability appears to be low in these soils, and may also reflect the low relative abundance of genes coding for phytate in these soils (Fig. 6; Figure S1, Supporting Information).

Increased concentrations of soil P in fertilized treatments compared with unfertilized treatments are consistent with previous studies under cropping (McLaughlin *et al.* 2011). However, the slight decrease in extractable total P for RockP under sorghum compared with P0 indicates that much of the fertilizer P remains undissolved (i.e. calcium phosphates) or transformed to a different soil P species that is insoluble in NaOH-EDTA. Pools of NaOH-EDTA extractable inorganic P in soil are considered to be those of aluminum and iron phosphates, and pools of P sorbed to mineral surfaces (Novais and Smyth 1999). Concentrations of extractable inorganic P increased in the RockP and TSP treatments compared with P0 for maize, which suggest much of the added fertilizer P was sorbed by the soil and unavailable for plant uptake. This would be consistent with the crop yield data, which remained unchanged for maize. However, concentrations of inorganic P increased to a lesser extent for TSP, and remained largely unchanged for Rock P, when compared with the P0 sorghum. It is likely that the exudation of low molecular weight organic acids by sorghum resulted in a greater mobilization of sorbed P, which could then be taken up by the crop (Jones 1998; Johnson and Loeppert 2005).

The principal mechanisms employed by plants in response to low-P bioavailability in soil are modulation of high-affinity P transporters and exudation or secretion of organic acids and phosphatases to liberate orthophosphate from inorganic and organic complexes, respectively. Root morphology modifications leading to an increase in fine roots capable of efficient mining of soil for P also enhance uptake and grain yield in tropical soils with low-P availability (Hufnagel *et al.* 2014). Root morphological changes, together with organic acid exudation and phosphatase secretion, can influence the abundance and species richness of microbial communities thought to aid plants in acquiring P from soil (López-Arredondo, Leyva-González and González-Morales 2014).

A diverse group of organisms were found associated with the rhizosphere of the crops in this study. Actinobacteria are well adapted to dry environments such as well-drained oxisols since they have evolved strategies, including sporulation and encystment, to survive extreme water stress (Soina *et al.* 2004; Mohammadipanah and Wink 2016), as well as low pH (Khan and

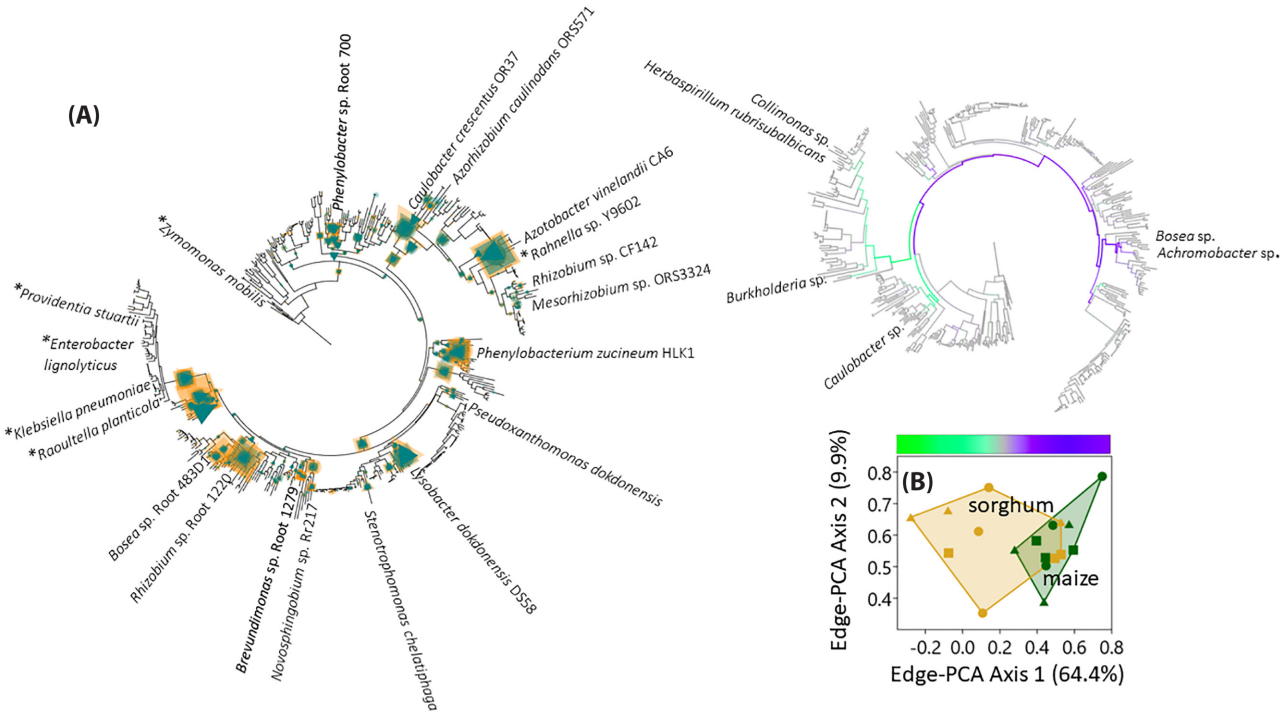

Figure 9. Phylogenetic comparison of NSAP class A gene ecotype assemblages in rhizospheres of maize (green placements and data points) and sorghum (yellow placements and data points) grown in Cerrado soil. **(A)** Phylogenetic placement of metagenome reads with homology to reference NSAP class A genes in soils receiving RockP (indicated with circular placements and data points), TSP (indicated with square placements and data points) or no phosphorus fertilization (P0—indicated with triangle placements and data points). Organisms harboring the NSAP class A genes with which ecotypes share homology are identified on branch tips of the maximum-likelihood gene reference phylogram. Placement symbol size is scaled to reflect relative abundance across the 18 samples. Asterisk (*) identifies reference genes described by Gandhi and Chandra (2012). **(B)** Ordination of NSAP class A assemblages shown in (A), exploiting the underlying phylogenetic nucleotide sequence structure (edge-PCA). Edges associated with large eigenvectors are shown in the associated color-coded phylogram, and organisms related to each branch are identified by taxonomic name. Branch color corresponds to the edge-PCA axis color scale. The arrow associates the color-coded phylogram with its corresponding edge-PCA axis. Gene assemblages associated with maize and sorghum are separated on edge-PCA axis 1.

Williams 1975). It is therefore not surprising to find that several dominant bacteria in the crop rhizospheres in these Cerrado soils were Actinobacteria. Similarly, it is also not unusual to identify several dominant Acidobacteria, which are particularly well adapted to oligotrophic, acidic soils (Kielak *et al.* 2016). Actinobacteria often harbor suites of enzymes necessary to degrade plant biomass and they are probably important for terrestrial carbon cycling (Lewin *et al.* 2016). The Gemmatimonadetes organism *Gemmatirosa kalamazoonesis* is a representative of a group of extremely abundant soil bacteria that are well adapted to arid conditions, constituting as much as 2% of global soil communities (DeBruyn *et al.* 2011). The bacterial communities in these soils therefore appears very typical of soil communities from around the world. Of the dominant archaeal species, two are dependent upon close association with other organisms. *Ca.* Prometheoarchaeum syntrophicum MK-D1 is a slow-growing anaerobic organism that degrades amino acids syntrophically in association with other archaea—*Halodesulfovibrio* and *Methanogenium* in the original co-cultures—through interspecies hydrogen (and/or formate) transfer (Imachi *et al.* 2020). A second mesothermophilic organism, *Ca.* Mancarchaeum acidiphilum MIA14, also degrades proteins and amino acids as part of an obligate partner-dependent lifestyle (Golyshina, Toshchakov and Makarova 2017) and its genome lacks any genes of the central carbohydrate metabolism pathways. Free-living *Ca.* Korarchaeum cryptofilum OPF8 grows heterotrophically, but also using a variety of peptide and amino acid degradation pathways (Elkins *et al.* 2008). Fungal communities were dominated by poorly studied organisms, none of which have been documented to have a mycorrhizal lifestyle. These included the bamboo-associating *Brunneoclavispora bambusae* and *Recurvomyces mirabilis*, a rock-inhabiting fungus of semi-arid environments (Selbmann *et al.* 2008). Several of the most abundant fungi exhibit biotrophy, including the obligate aphid pathogen *Conidiobolus obscurus* (Wang *et al.* 2018) and *Cornuvesica acuminata*, *Dactylidispora singaporensis* and *D. ellipsospora* all of which are mycoparasites and typically isolated from soils (Marin-Felix *et al.* 2018). Identification of the Mucormycete *Gongronella orasabula* is potentially significant for P acquisition by crops in these soils as a congener, *Gongronella* sp. w5, is a putative biotrophic fungus that may promote plant growth by secreting organic acids, facilitating plant phosphate acquisition (Dong *et al.* 2018).

Despite the limited difference in rhizosphere communities associated with the crops based on small subunit ribosomal RNA (SSU rRNA) gene KR distance metrics, bacterial, archaeal and fungal community median PD was consistently greater in maize rhizospheres than sorghum (Fig. 4). In stark contrast, all phosphohydrolase genes studied in detail were both more abundant and exhibited greater PD in sorghum rhizospheres (Fig. 6). This is a salient finding; it demonstrates that the abundance and PD of genes coding for these important enzymes respond independently of community marker genes. This phenomenon has been observed before in cultivated soils growing winter wheat (Neal

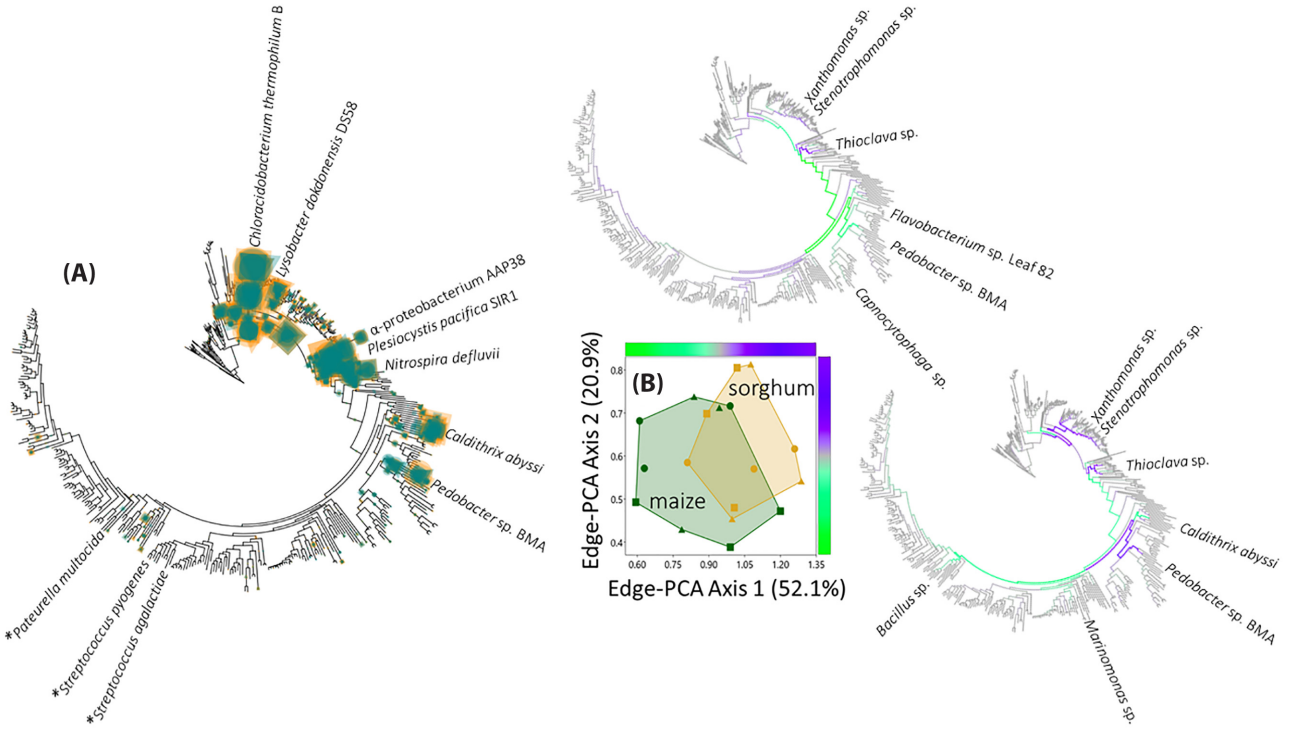

Figure 10. Phylogenetic comparison of NSAP class C gene ecotype assemblages in rhizospheres of maize (green placements and data points) and sorghum (yellow placements and data points) grown in Cerrado soil. **(A)** Phylogenetic placement of metagenome reads with homology to reference NSAP class C genes in soils receiving RockP (indicated with circular placements and data points), TSP (indicated with square placements and data points) or no phosphorus fertilization (P0—indicated with triangle placements and data points). Organisms harboring the NSAP class A genes with which ecotypes share homology are identified on branch tips of the maximum-likelihood gene reference phylogram. Placement symbol size is scaled to reflect relative abundance across the 18 samples. Asterisk (*) identifies reference genes described by Gandhi and Chandra (2012). **(B)** Ordination of NSAP class C assemblages shown in (A), exploiting the underlying phylogenetic nucleotide sequence structure (edge-PCA). Gene assemblages associated with maize and sorghum are separated on both edge-PCA axes 1 and 2. Edges associated with large eigenvectors are shown in the associated color-coded phylograms, and organisms related to each branch are identified by taxonomic name. Branch color corresponds to edge-PCA axis color scale. The arrows associate each color-coded phylogram with its corresponding edge-PCA axis.

and Glendining 2019). Comparing phosphohydrolase genes in UK agricultural soils maintained at a minimum soil pH of 7.0–7.5 with calcium carbonate addition to promote plant health with the more acidic Cerrado soils suggests that the general phylogenetic diversity of genes differs between the soils: specifically, the estimated mean PD of alkaline phosphatase *phoX* genes is greater than either of the NSAP classes in UK agricultural soil (Supplementary Fig. 2 of Neal and Glendining 2019), but the three genes have similar estimated mean PD in Cerrado soils (Figure S1, Supporting Information). Observations of variable gene diversity in soils from a wide variety of geographical locations with a wide variety of P chemistry and availability have been observed before (Ragot *et al.* 2017). This variability may simply reflect the prevailing pH in UK and Cerrado soils. However, Neal and Glendining (2019) noted that alkaline phosphatases PhoD and PhoX and the βPPhy enzymes all require calcium as a cofactor and low calcium bioavailability may be associated with an increase in PHO genes coding for enzymes that do not require calcium cofactor, such as NSAPs. Cerrado soils are characteristically low in bioavailable calcium (Lopes and Guimarães 2016) and the increased NSAP diversity observed in these soils would be consistent with calcium exerting a degree of influence upon wider phosphohydrolase gene diversity.

It is evident that neither the levels [P0 vs (RockP, TSP)] nor the quality (RockP vs TSP) of P fertilization exerted any significant influence upon the abundance or PD of phosphohydrolase genes. It is well recognized that plants release complex mixtures of relatively structurally simple compounds from their roots into the surrounding soil, which may attract quite distinct communities of microorganisms to the rhizosphere (Neal *et al.* 2012; Schlemper, Leite and Lucheta 2017; Hu *et al.* 2018; Miller *et al.* 2019). These microorganisms can increase orthophosphate supply to plants by hydrolysis of organic P through the action of phosphatases, especially phytases (Richardson and Simpson 2011) or by RockP solubilization through organic acid production (Mendes, de Freitas and Pereira 2014). Both maize and sorghum are also known to secrete phosphatase enzymes into the rhizosphere (Furlani *et al.* 1984; Machado and Furlani 2004). We only included rhizosphere soil communities here, so cannot comment on how they differ from the background soil communities. However, if rhizosphere selection occurred it is evident that maize and sorghum attract and support phylogenetically similar communities. It is then hard to reconcile the observed increases in abundance and PD of phosphohydrolase genes with the limited changes in community structure: we conjecture that it is in fact genes themselves that become more abundant because they confer competitive advantage to individual cells rather than species within the confines of the sorghum rhizosphere, where the genes are collectively both more abundant and phylogenetically diverse. This would require lateral transfer of genes between community members (Maheshwari *et al.* 2017). Inspection of the PHO gene ecotypes identified as responsive to the different crop types by edge-PCA (Figs 7–10) corroborates this notion: many of the responsive ecotypes form clades of closely related phosphohydrolase gene sequences that are found in phylogenetically distinct

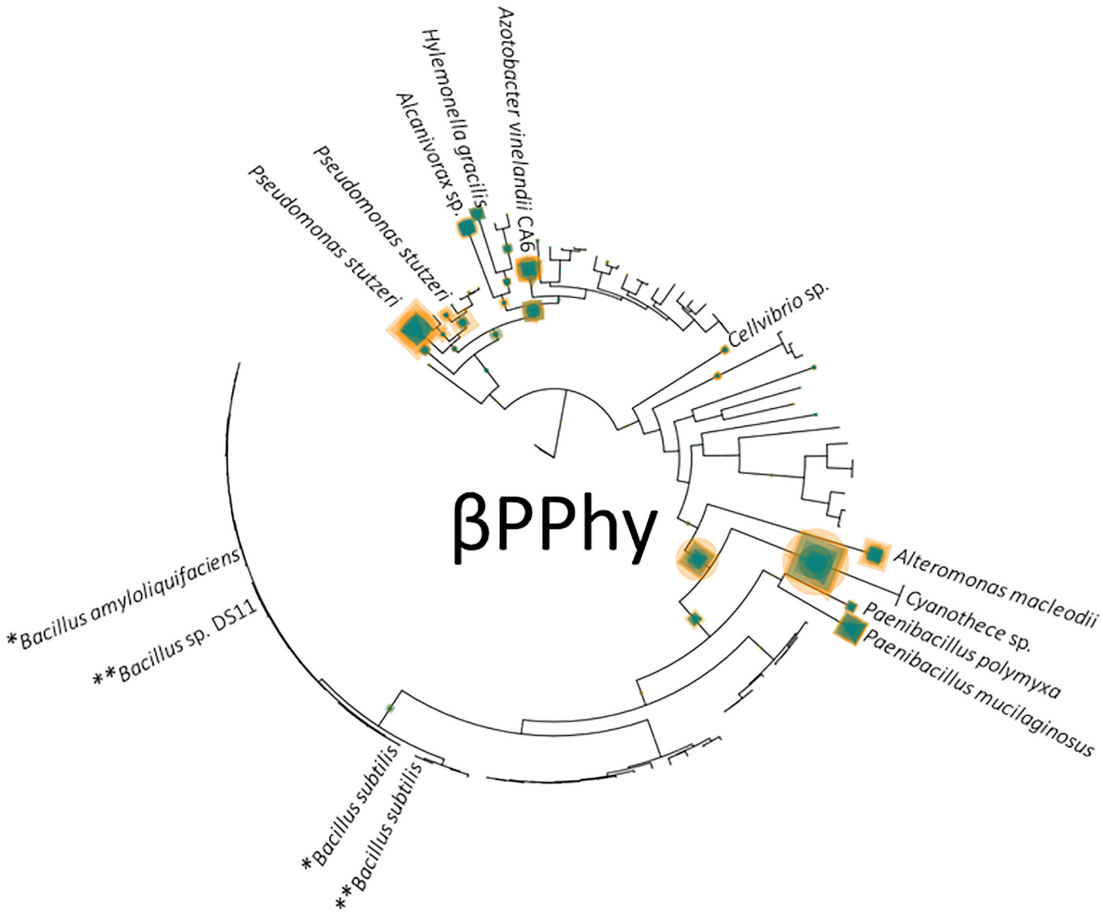

Figure 11. Phylogenetic comparison of beta propeller phytase (βPPhy) gene ecotype assemblages in rhizospheres of maize (green placements and data points) and sorghum (yellow placements and data points) grown in Cerrado soil. Phylogenetic placement of metagenome reads with homology to reference βPPhy genes in soils receiving RockP (indicated with circular placements and data points), TSP (indicated with square placements and data points) or no phosphorus fertilization (P0—indicated with triangle placements and data points). Organisms harboring the βPPhy genes with which ecotypes share homology are identified on branch tips of the maximum-likelihood gene reference phylogram. Placement symbol size is scaled to reflect relative abundance across the 18 samples. Asterisk (*) identifies reference genes described by Lim *et al.* (2007); (**) identifies SWISS-PROT accessions.

organisms—most commonly from different classes of the proteobacteria. For example, the phylogenetically close *phoD* gene sequences found in the α-proteobacteria *Sphingopyxis* and *Asticcacaulis* and the β-proteobacteria *Ralstonia* and *Cupriavidus* are identified as associating more with the sorghum rhizosphere (Fig. 7), or the phylogenetically close NSAPa gene sequences found in the α-proteobacterium *Bosea* and β-proteobacterium *Achromobacter* that associate more with maize (Fig. 9).

Despite reduced solubility, RockP can be an effective P fertilizer in tropical environments, especially regarding the surficial reactions between the mineral and soil solution, which are intensified at the temperatures and humidity in tropical soils (Trabelsi *et al.* 2017). However, depending on the properties of RockP, soil, climatic conditions, crops and management practices, up to four years of annual application is required for RockP to be as effective as soluble phosphates (Ghani, Rajan and Lee 1994). Our study was performed in the second year of continuous RockP application, suggesting it is feasible in terms of crop yield to use RockP as an alternative P source than soluble P fertilizers over the long term. However, in soils with high P adsorption and low ion exchange capacities, such as the Brazilian Oxisols studied here, short-term direct use of RockP as fertilizers for annual crops may be less economically viable. One option to overcome this would be to use partially acidulated rock phosphates, and inocula of selected microorganisms, such as the ones harboring gene ecotypes identified in this study, or selective breeding of crops with an enhanced capacity to attract beneficial microorganisms to the rhizosphere (de Sousa *et al.* 2020; Velloso *et al.* 2020).

ACKNOWLEDGMENTS

The authors would like to thank Dr Rene´ Verel of the Laboratory of Inorganic Chemistry (Ho¨nngerberg, ETH Zu¨rich) and Dr Laurie Paule Scho¨nholzer of the Group of Plant Nutrition (Eschikon, ETH Zu¨rich) for technical assistance. Authentic samples of *myo-*, *scyllo-*, *neo-* and *chiro*-inositol hexakisphosphate were acquired from the original collections of Dr Dennis Cosgrove and Dr Max Tate.

SUPPLEMENTARY DATA

Supplementary data are available at *FEMSEC* online.

FUNDING

This work was supported by the Empresa Brasileira de Pesquisa Agropecuária—EMBRAPA (Grant No. 12.14.10.003.00.00)

and a Biotechnology and Biological Sciences Research Council (BBSRC)/Newton-funded UK–Brazil Alliance for Sustainable Agriculture award. ALN and DH are supported by the BBSRC-funded Soil to Nutrition strategic programme (BBS/E/C/000I0310) and the Natural Environment Research Council and BBSRC as part of the Achieving Sustainable Agricultural Systems research programme (NE/N018125/1 LTS-M). MLC is a recipient of a research fellowship from Coordenação de Aperfeiçoamento de Pessoal de Nível Superior—CAPES.

REFERENCES

Anderson MJ, ter Braak C. Permutation tests for multi-factorial analysis of variance. *J Stat Comput Simul* 2003;**73**:85–113.

Anderson MJ. Distance-based tests for homogeneity of multivariate dispersions. *Biometrics* 2006;**62**:245–53.

Bakker MG, Chaparro JM, Manter DK *et al*. Impacts of bulk soil microbial community structure on rhizosphere microbiomes of *Zea mays*. *Plant Soil* 2015;**392**:115–26.

Barbera P, Kozlov AM, Czech L *et al*. EPA-ng: massively parallel evolutionary placement of genetic sequences. *Syst Biol* 2019;**68**:365–69.

Bolger AM, Lohse M, Usadel B. Trimmomatic: a flexible trimmer for Illumina sequence data. *Bioinformatics* 2014;**30**:2114–20.

Bowman JS, Ducklow HW. Microbial communities can be described by metabolic structure: a general framework and application to a seasonally variable, depth-stratified microbial community from the coastal West Antarctic Peninsula. *PLoS One* 2015;**10**:e0135868.

Cade-Menun B, Preston C. A comparison of soil extraction procedures for ^{31}P NMR spectroscopy. *Soil Sci* 1996;**161**:770–85.

Camenzind T, Hättenschwiler S, Treseder K *et al*. Nutrient limitation of soil microbial processes in tropical forests. *Ecol Monog* 2018;**88**:4–21.

Cardoso IM, Kuyper TW. Mycorrhizas and tropical soil fertility. *Agric Ecosyst Environ* 2006;**116**:72–84.

Chien SH, Prochnow LI, Tu S *et al*. Agronomic and environmental aspects of phosphate fertilizers varying in source and solubility: an update review. *Nutr Cycl Agroecosyst* 2011;**89**:229–55.

Czech L, Stamatakis A. Scalable methods for analysing and visualizing phylogenetic placement of metagenomic samples. *PLoS One* 2019;**14**:e0217050.

DeBruyn JM, Nixon LT, Fawaz MN *et al*. Global biogeography and quantitative seasonal dynamics of Gemmatimonadetes in soil. *Appl Environ Microbiol* 2011;**77**:6295–300.

de Sousa SM, de Oliveira CA, Andrade DL *et al*. Tropical *Bacillus* strains inoculation enhances maize root surface area, dry weight, nutrient uptake and grain yield. *J Plant Growth Regul* 2020, DOI: 10.1007/s00344-020-10146-9.

Dong Y, Sun Q, Zhang Y *et al*. Complete genome of *Gongronella* sp. w5 provides insight into its relationship with plant. *J Biotechnol* 2018;**286**:1–4.

Doolette AL, Smernik RJ, Dougherty WJ. Overestimation of the importance of phytate in NaOH–EDTA soil extracts as assessed by ^{31}P NMR analyses. *Org Geochem* 2011;**42**:955–64.

Doolette AL, Smernik RJ, Dougherty WJ. Rapid decomposition of phytate applied to a calcareous soil demonstrated by a solution ^{31}P NMR study. *Eur J Soil Sci* 2010;**61**:563–75.

Eddy S. A new generation of homology search tools based on probabilistic inference. *Genome Inform* 2009;**23**:205–11.

Edwards J, Johnson C, Santos-Medellín C *et al*. Structure, variation, and assembly of the root-associated microbiomes of rice. *Proc Natl Acad Sci USA* 2015;**112**:911–20.

Elkins JG, Podar M, Graham DE *et al*. A korarchaeal genome reveals insights into the evolution of the Archaea. *Proc Natl Acad Sci USA* 2008;**105**:8102–7.

Embrapa. *Centro Nacional de Pesquisa de Solos. Manual de métodos e análise de solo*, 2nd edn. Rio de Janeiro: CNPS, 1997, 212.

Evans SN, Matsen FA. The phylogenetic Kantorovich–Rubinstein metric for environmental sequence samples. *J R Stat Soc Series B Stat Methodol* 2012;**74**:569–92.

FAO. *The state of food and agriculture. Moving forward on food loss and waste reduction*. 2019. http://www.fao.org/3/ca6030en/ca6030en.pdf.

Furlani A, Clark R, Maranville J *et al*. Root phosphatase activity of sorghum genotypes grown with organic and inorganic sources of phosphorus. *J Plant Nutr* 1984;**7**:1583–95.

Gandhi NU, Chandra SB. A comparative analysis of three classes of bacterial non-specific acid phosphatases and archaeal phosphoesterases: evolutionary perspective. *Acta Informatica Medica* 2012;**20**:167–73.

Garland G, Bünemann EK, Oberson A *et al*. Phosphorus cycling within soil aggregate fractions of a highly weathered tropical soil: a conceptual model. *Soil Biol Biochem* 2018;**116**:91–8

Gaunt MW, Turner SL, Rigottier-Gois L *et al*. Phylogenies of *atpD* and *recA* support the small subunit rRNA-based classification of rhizobia. *Int J Syst Evol Microbiol* 2001;**51**:2037–48.

George TS, Giles CD, Menezes-Blackburn D *et al*. Organic phosphorus in the terrestrial environment: a perspective on the state of the art and future priorities. *Plant Soil* 2018;**427**:191–208.

Ghani A, Rajan SSS, Lee A. Enhancement of phosphate rock solubility through biological processes. *Soil Biol Biochem* 1994;**26**:127–36.

Golyshina OV, Toshchakov S, Makarova KS. 'ARMAN' archaea depend on association with euryarchaeal host in culture and *in situ*. *Nat Commun* 2017;**8**:60.

Gomes EA, Lana UGP, Quensen JF *et al*. Root-associated microbiome of maize genotypes with contrasting phosphorus use efficiency. *Phytobiomes J* 2018;**2**:129–37.

Hammer Ø, Harper D, Ryan P. PAST: paleontological statistics software package for education and data analysis. *Palaeontol Electron* 2001;**4**:1–9.

Holland BS, Copenhaver MD. An improved sequentially rejective Bonferroni test procedure. *Biometrics* 1987;**43**:417–23.

Howard E, Shulei F, Erin M *et al*. Abundant and diverse bacteria involved in DMSP degradation in marine surface waters. *Environ Microbiol* 2008;**10**:2397–410.

Hufnagel B, de Sousa SM, Assis L *et al*. Duplicate and conquer: multiple homologs of *PHOSPHORUS-STARVATION TOLERANCE1* enhance phosphorus acquisition and sorghum performance on low-phosphorus soils. *Plant Physiol* 2014;**166**:659–77.

Hu L, Robert CAM, Cadcot S *et al*. Root exudate metabolites drive plant-soil feedbacks on growth and defense by shaping the rhizosphere microbiota *Nat Commun* 2018;**9**:2738.

Imachi H, Nobu MK, Nakahara N *et al*. Isolation of an archaeon at the prokaryote–eukaryote interface. *Nature* 2020;**577**:519–25.

Johnson SE, Loeppert RH. Role of organic acids in phosphate mobilization from iron oxide. *Soil Sci Soc Am J* 2005;**70**:222–34.

Jones D. Organic acids in the rhizosphere: a critical review. *Plant Soil* 1998;**205**:25–44.

Katoh K, Standley DM. MAFFT Multiple Sequence Alignment Software Version 7: improvements in performance and usability. *Mol Biol Evol* 2013;**30**:772–80.

Khan MR, Williams ST. Studies on the ecology of actinomycetes in soil. VIII. Distribution and characteristics of acidophilic actinomycetes. *Soil Biol Biochem* 1975;**7**:345–48.

Kielak AM, Barreto CC, Kowalchuk GA *et al*. The ecology of Acidobacteria: moving beyond genes and genomes. *Front Microbiol* 2016;**7**:744.

Letunic I, Bork P. Interactive Tree of Life (iTOL) v3: an online tool for the display and annotation of phylogenetic and other trees. *Nucleic Acids Res* 2016;**44**:242–5.

Lewin GR, Carlos C, Chevrette MG *et al*. Evolution and ecology of Actinobacteria and their bioenergy applications. *Annu Rev Microbiol* 2016;**70**:235–54.

Lim BL, Yeung P, Cheng C *et al*. Distribution and diversity of phytate-mineralizing bacteria. *ISME J* 2007;**1**:321–30.

Li X, Rui J, Xiong J *et al*. Functional potential of soil microbial communities in the maize rhizosphere. *PLoS One* 2014;**9**:e112609.

Loganathan P, Hedley MJ, Bolan NS *et al*. Field evaluation of the liming value of two phosphate rocks and their partially acidulated products after 16 years of annual application to grazed pasture. *Nutr Cycl Agroecosyst* 2005;**72**:287–97.

Lopes AR, Guimarães GLR. A career perspective on soil management in the Cerrado Region of Brazil. I n: *Advances in Agronomy*, Vol. 137. San Diego: Elsevier, 2016, 1–72.

López-Arredondo D, Leyva-González M, González-Morales S. Phosphate nutrition: improving low-phosphate tolerance in crops. *Ann Rev Plant Biol* 2014;**65**:95–123.

Machado CTT, Furlani AMC. Root phosphatase activity, plant growth and phosphorus accumulation of maize genotypes. *Sci Agric* 2004;**61**:216–23.

Maheshwari M, Abulreesh HH, Khan MS *et al*. Horizontal gene transfer in soil and the rhizosphere: impact on ecological fitness of bacteria. In: Meena V, Mishra P, Bisht J, Pattanayak A (eds). *Agriculturally Important Microbes for Sustainable Agriculture*. Singapore: Springer, 2017.

Majumdar A, Ghatak A, Ghosh RK. Identification of the gene for the monomeric alkaline phosphatase of *Vibrio cholerae* serogroup O1 strain. *Gene* 2005;**344**:251–8.

Margenot AJ, Singh BR, Rao IM *et al*. Phosphorus fertilization and management in soils of Sub-Saharan Africa. In: *Soil Phosphorus (Advances in Soil Science)*, CRC Press, 2016, 151–208.

Marin-Felix Y, Guarro J, Ano-Lira JF *et al*. Melanospora (Sordariomycetes, Ascomycota) and its relatives. *MycoKeys* 2018;**44**:81–122.

Marschner P, Solaiman Z, Rengel Z. Rhizosphere properties of Poaceae genotypes under P-limiting conditions. *Plant Soil* 2006;**283**:11–24.

Matsen FA, Evans SN. Edge principal components and squash clustering: using the special structure of phylogenetic placement data for sample comparison. *PLoS One* 2013;**8**:e56859.

Matsen FA, Kodner RB, Armbrust EV. pplacer: linear time maximum-likelihood and Bayesian phylogenetic placement of sequences onto a fixed reference tree. *BMC Bioinformatics* 2010;**11**:538.

McCoy CO, Matsen FA. Abundance-weighted phylogenetic diversity measures distinguish microbial community states and are robust to sampling depth. *PeerJ*. 2013;**1**:157.

McLaren TI, Smernik RJ, McLaughlin MJ *et al*. Complex forms of soil organic phosphorus: a major component of soil phosphorus. *Environ Sci Technol* 2015;**49**:13238–45.

McLaren TI, Verel R, Frossard E. The structural composition of soil phosphomonoesters as determined by solution ^{31}P NMR spectroscopy and transverse relaxation (T2) experiments. *Geoderma* 2019;**345**:31–37.

McLaughlin MJ, McBeath TM, Smernik R *et al*. The chemical nature of P accumulation in agricultural soils—implications for fertiliser management and design: an Australian perspective. *Plant Soil* 2011;**349**:69–87.

McMurdie PJ, Holmes S. Waste not, want not: why rarefying microbiome data is inadmissible. *PLoS Comput Biol* 2014;**10**:e1003531.

Mendes GO, de Freitas ALM, Pereira OL. Mechanisms of phosphate solubilization by fungal isolates when exposed to different P sources. *Ann Microbiol* 2014;**64**:239–49.

Miller SB, Heuberger AL, Broeckling CD *et al*. Non-targeted metabolomics reveals Sorghum rhizosphere-associated exudates are influenced by the belowground interaction of substrate and Sorghum genotype. *Int J Mol Sci* 2019;**20**:431.

Mohammadipanah F, Wink J. Actinobacteria from arid and desert habitats: diversity and biological activity. *Front Microbiol* 2016;**6**:1541.

Monds R, Newell P, Schwartzman J *et al*. Conservation of the Pho regulon in *Pseudomonas fluorescens* Pf0-1. *Appl Environ Microbiol* 2006;**72**:1910–24.

Mota D, Faria F, Gomes EA *et al*. Bacterial and fungal communities in bulk soil and rhizospheres of aluminum-tolerant and aluminum-sensitive maize *Zea mays* L. lines cultivated in unlimed and limed Cerrado soil, *J Microbiol Biotechnol* 2008;**18**:805–14.

Naumann G, Alfieri L, Wyser K *et al*. Global changes in drought conditions under different levels of warming. *Geophys Res Lett* 2018;**45**:3285–96.

Neal AL, Ahmad S, Gordon-Weeks R *et al*. Benzoxazinoids in root exudates of maize attract *Pseudomonas putida* to the rhizosphere. *PLoS One* 2012;**7**:e35498.

Neal AL, Blackwell M, Akkari E *et al*. Phylogenetic distribution, biogeography and the effects of land management upon bacterial non-specific acid phosphatase gene diversity and abundance. *Plant Soil* 2017b;**427**:175–89.

Neal AL, Glendining MJ. Calcium exerts a strong influence upon phosphohydrolase gene abundance and phylogenetic diversity in soil. *Soil Biol Biochem* 2019;**139**:107613.

Neal AL, Rossmann M, Brearley C *et al*. Land-use influences phosphatase gene microdiversity in soils. *Environ Microbiol* 2017a;**19**:2740–53.

Ngumbi E, Kloepper J. Bacterial-mediated drought tolerance: current and future prospects. *Appl Soil Ecol* 2016;**105**:109–25.

Nipperess DA, Matsen FA. The mean and variance of phylogenetic diversity under rarefaction. *Methods Ecol Evol* 2013;**4**:566–72.

Novais RF, Smyth TJ. *Fósforo no solo e nas plantas em condições tropicais*. Viçosa, MG, Brasil: Universidade Federal de Viçosa, 1999, 309.

Ragot SA, Kertesz MA, Mészáros E *et al*. Soil *phoD* and *phoX* alkaline phosphatase gene diversity responds to multiple environmental factors, *FEMS Microbiol Ecol* 2017;**93**:212.

Reusser JE, Verel R, Frossard E *et al*. Quantitative measures of *myo*-IP_6 in soil using solution ^{31}P NMR spectroscopy and spectral deconvolution fitting including a broad signal. *Environ Sci: Processes Impacts* 2020;**22**:1084–94.

Rice P, Longden I, Bleasby A. EMBOSS: the European molecular biology open software suite. *Trends Genet* 2000;**16**:276–87.

Richardson AE, Simpson RJ. Soil microorganisms mediating phosphorus availability update on microbial phosphorus. *Plant Physiol* 2011;**156**:989–96.

Santos HG, Jacomine PKT, Anjos LHC *et al*. *Sistema brasileiro de classificação de solos. 3. Ed*, Brasília, DF: Embrapa, 2013, 353.

Santos S, Ochman H. Identification and phylogenetic sorting of bacterial lineages with universally conserved genes and proteins. *Environ Microbiol* 2004;**6**:754–59.

Schlemper TR, Leite MFA, Lucheta AR. Rhizobacterial community structure differences among sorghum cultivars in different growth stages and soils. *FEMS Microbiol Ecol* 2017;**93**:fix096.

Selbmann L, de Hoog GS, Zucconi L *et al.* Drought meets acid: three new genera in a dothidealean clade of extremotolerant fungi. *Stud Mycol* 2008;**61**:1–20.

Sharma N, Singhvi R. Effects of chemical fertilizers and pesticides on human health and environment: a review. *Int J Agric Environ Biotechnol* 2017;**10**:675–79.

Silva UC, Medeiros JD, Leite LR *et al.* Long-term rock phosphate fertilization impacts the microbial communities of maize rhizosphere. *Front Microbiol* 2017;**8**:1266.

Soina VS, Mulyukin AL, Demkina EV *et al.* The structure of resting bacterial populations in soil and subsoil permafrost. *Astrobiology* 2004;**4**:345–58.

Stamatakis A. RAxML version 8: a tool for phylogenetic analysis and post-analysis of large phylogenies. *Bioinformatics* 2014;**30**:1312–3.

Tabatabai M. Soil enzymes. In: Weaver RW, Angle S, Bottomley P *et al.* (eds). *Methods of Soil Analysis: Part 2 Microbiological and Biochemical Properties*. Madison, WI: SSSA Book Series, 1994, 775–34.

Trabelsi D, Cherni AE, Ben Zineb A *et al.* Fertilization of *Phaseolus vulgaris* with the Tunisian rock phosphate affects richness and structure of rhizosphere bacterial communities. *Appl Soil Ecol* 2017;**114**:1–8.

Vega NWO. A review on beneficial effects of rhizosphere bacteria on soil nutrient availability and plant nutrient uptake. *Rev Fac Nac Agron Medellín* 2007;**60**:3621–43.

Velloso CCV, Oliveira CA, Gomes EA *et al.* Genome-guided insights of tropical *Bacillus* strains efficient in maize growth promotion. *FEMS Microbiol Ecol* 2020;**96**:fiaa157.

Vold RL, Waugh JS, Klein MP *et al.* Measurement of spin relaxation in complex systems. *J Chem Phys* 1968;**48**:3831–2.

Wang J, Zhou X, Guo K *et al.* Transcriptomic insight into pathogenicity-associated factors of *Conidiobolus obscurus*, an obligate aphid-pathogenic fungus belonging to Entomopthoromycota. *Pest Manag Sci* 2018;**74**:1677–86.

Wu JR, Shien JH, Shieh HK *et al.* Cloning of the gene and characterization of the enzymatic properties of the monomeric alkaline phosphatase (PhoX) from *Pasteurella multocida* strain X-73. *FEMS Microbiol Lett* 2006;**267**:113–20.